A review on fiber optic sensors for rebar corrosion monitoring in RC structures

Fujian Tang[1,*], Guoshuai Zhou[1], Hong-Nan Li[1], Els Verstrynge[2]

[1]School of Civil Engineering, Dalian University of Technology, DL 116024, China
[2]Department of Civil Engineering, KU Leuven, Kasteelpark Arenberg 40, 3001 Leuven, Belgium

Abstract. Reinforcement steel corrosion is one of the major causes of premature deterioration of concrete structures in marine environments or subjected deicing salts. Steel corrosion causes economic loss and even results in structural collapse and consequently loss of human life. Various optical fiber sensors have been proposed to monitor steel rebar corrosion in concrete structures over the past two decades due to light weight, compactness, small size, immunity to electromagnetic interference, and capacity of being multiplexed into a sensor network. This study presents a state-of-the-art review of optical fiber sensors for corrosion monitoring of reinforcement steel in concrete structures with emphasis on sensing principle and performance parameters including measurand, sensitivity, monitoring range and service life. The optical fiber corrosion sensors reviewed in this study mainly include fiber Bragg grating (FBG) based corrosion sensors, long-period fiber grating (LPFG) corrosion sensors, extrinsic Fabry-Perot interferometer (EFPI) corrosion sensors, Brillouin backscattering-based distributed fiber optic corrosion sensors, optical frequency domain reflectometry (OFDR) corrosion sensors, and other fiber optic corrosion sensors. This review aims to clarify performance and limitations of fiber optic sensors for reinforcement steel corrosion monitoring in concrete for the purpose of providing a foundation for future research and engineering applications.

Keywords: Optical fiber sensors; corrosion monitoring; reinforced concrete; refractive index.

1. Introduction

Reinforced concrete (RC) has been a widely used construction material for civil infrastructures such as buildings, bridges, dams, tunnels and airports across the world due to easy availability of its constituents

* Corresponding to: Prof. Fujian Tang, E-Mail: ftang@dlut.edu.cn

such as water, sand, stone and cement. The design service life of reinforced concrete structures ranges from 30 to 120 years depending on the type and importance of the structures (e.g., 30-50 years for port infrastructures, 100-120 years for bridges) [1, 2]. However, premature deterioration often occurs in RC structures located in aggressive environment or subjected to attack of corrosive chemicals. For examples, corrosion of reinforcement steel is one of the main causes of premature deterioration of RC structures in marine environment or in cold regions with use of deicing salts. Corrosion causes concrete cover cracking, mechanical degradation of steel reinforcement, bond loss between concrete and reinforcement steel, and carrying capacity reduction of structural components and/or structural systems. Moreover, corrosion of civil infrastructures brings direct and indirect economic loss and even poses threats to human life. In China, the corrosion cost for civil infrastructure such as roads, highway bridges, ports and piers was estimated to be 65 billion RMB in 2014 [3]. The direct corrosion cost for highway bridges was estimated to be $13.6 billion in the U.S. in 2013, and the indirect cost was estimated to be 10 times greater than the direct cost due to traffic delay or loss of productivity [4]. A cross-sectional reduction of the stay cable steel due to corrosion is also one of the causes of the Morandi bridge collapse in Italy in 2018, in which 43 people were killed [5]. The collapse of a 12-story condominium near Miami on June 24, 2021 had a death toll of nearly 100 people. Inspection revealed that extensive corrosion had occurred in columns at the building's foundations [6]. Therefore, it is important to develop sensors or sensing instruments to monitor the corrosion of steel reinforcement in RC structures for providing early alarm of potential collapse. In addition, the corrosion data collected by the sensors can be used for timely safety assessment and decision-making on maintenance strategies.

Techniques to monitor reinforcement steel corrosion in concrete structures can be broadly divided into two categories: electrochemical and non-electrochemical (or physical) methods. Electrochemical techniques include half-cell potential, linear polarization resistance, electrochemical impedance spectroscopy, galvanostatic pulse, and electrochemical noise [7-10]. Non-electrochemical techniques include acoustic emission, ultrasonic testing, ultrasonic guided waves, magnetic or electromagnetic apparatus, x-ray scanning and computer tomography (XCT), (surface) crack monitoring, radio-frequency identification, and so on [11-15]. Each technique has its advantages and disadvantages. For example, open-circuit potential is the most widely used nondestructive technique for corrosion monitoring of reinforcement steel in concrete. However, it can only give the probability of corrosion instead of providing some quantitative information [7, 9]. XCT is a nondestructive method and can be employed to monitor morphology of steel corrosion as well as corrosion-induced concrete internal cracking. However, it is not suitable for on-site application of real-size structures [14].

Due to their small size, light weight, corrosion resistance, flexibility, immunity to electromagnetic interference, and capability of being multiplexed in a network, optical fibers have been used for multiple sensing purposes, and various fiber optic sensor types have been proposed for physical, chemical and biological sensing over the past three decades [16, 17]. In the meantime, many optical fiber sensors have also been developed and investigated for corrosion monitoring of steel reinforcement in RC structures, and different optical fiber corrosion sensor monitors corrosion with different sensing principle. Recently, a review on optical fiber corrosion sensors has been published focusing on the application stage in the whole service life of structures [18]. However, the performance parameters including sensitivity, monitoring range, service life, which are very important parameters for a sensor, have not been compared and discussed, and are the focus of current paper. Moreover, a timeline of fiber optic corrosion sensor development has been created as a foundation for future development.

In this paper, a state-of-the-art review of optical fiber sensors for corrosion monitoring of steel rebars in concrete structures is presented with emphasis on their performance parameters. The work is organized as follows: firstly, the timeline of fiber optic corrosion sensors proposed over the past two decades is created for a better understanding of the development history of fiber optic sensors for corrosion monitoring of reinforcement steel in concrete structures. Secondly, the fiber optic corrosion sensors are divided into six categories based on their different sensing principles: fiber Bragg grating (FBG) corrosion sensors, long-period fiber grating (LPFG) corrosion sensors, extrinsic Fabry-Perot interferometer (EFPI) -based corrosion sensors, Brillouin backscattering-based distributed fiber optic corrosion sensors and optical frequency domain reflectometry (OFDR) corrosion sensors, and other fiber optic corrosion sensors. The corrosion monitoring principle and performance parameters are discussed and analyzed. Thirdly, utilization of monitoring data obtained from these fiber optic corrosion sensors are discussed. Fourthly, perspective and challenges of fiber optic corrosion sensors for reinforced concrete structures are discussed. Finally, the paper ends with conclusions.

2. Timeline of fiber optic corrosion sensors development

The first use of optical fibers for sensor purpose dates back to 1960s, when a patent was filed based on free space optics [19]. About 10 years later, the first intrinsic fiber optic sensor was proposed for mechanical measurements. However, it could not yet be deployed in operating structures [19]. Starting in 1990s, various fiber optic sensors have been proposed and developed for monitoring physical, chemical, strain, temperature, pressure and more, especially with the development of the grating inscription technique [20]. Two of the most widely used fiber optic sensors are fiber Bragg grating (FBG) sensors and long period fiber grating (LPFG) sensors [21]. However, these sensors are point sensing which limits their application in large-scale structures. In the early 2000s, distributed fiber optics sensors based on Rayleigh, Brillouin and Raman scattering started to appear for distributed sensing of temperature, vibration, strain, and so on [22].

To the best of the authors' knowledge, the first use of fiber optic sensors for corrosion monitoring of civil structures dates back to 1990s, when a fiber optic sensor was proposed to monitor steel structure corrosion [23]. Since then, various fiber optic sensors or sensing instruments have been proposed to monitor steel corrosion in civil infrastructures. Figure 1 shows the timeline of fiber optic sensors for corrosion monitoring of steel reinforcement in reinforced concrete structures. It can be seen that the majority of fiber optic sensors for corrosion monitoring of steel reinforcement in concrete is proposed over the past ten years. These fiber optic corrosion sensors are based on different operating principles and can be classified as point corrosion sensing (FBG, LPFG, EFPI) and distributed corrosion sensing (BOTDR/A, OFDR). The working principle, corrosion monitoring principle and performance of these fiber optic corrosion sensors will be discussed in detail in the next sections in following order: FBG fiber corrosion sensors, LPFG fiber corrosion sensors, EFPI fiber corrosion sensors, Brillouin backscattering-based distribute fiber optic corrosion sensors, Rayleigh backscattering based fiber optic corrosion sensors, and other fiber corrosion sensors.

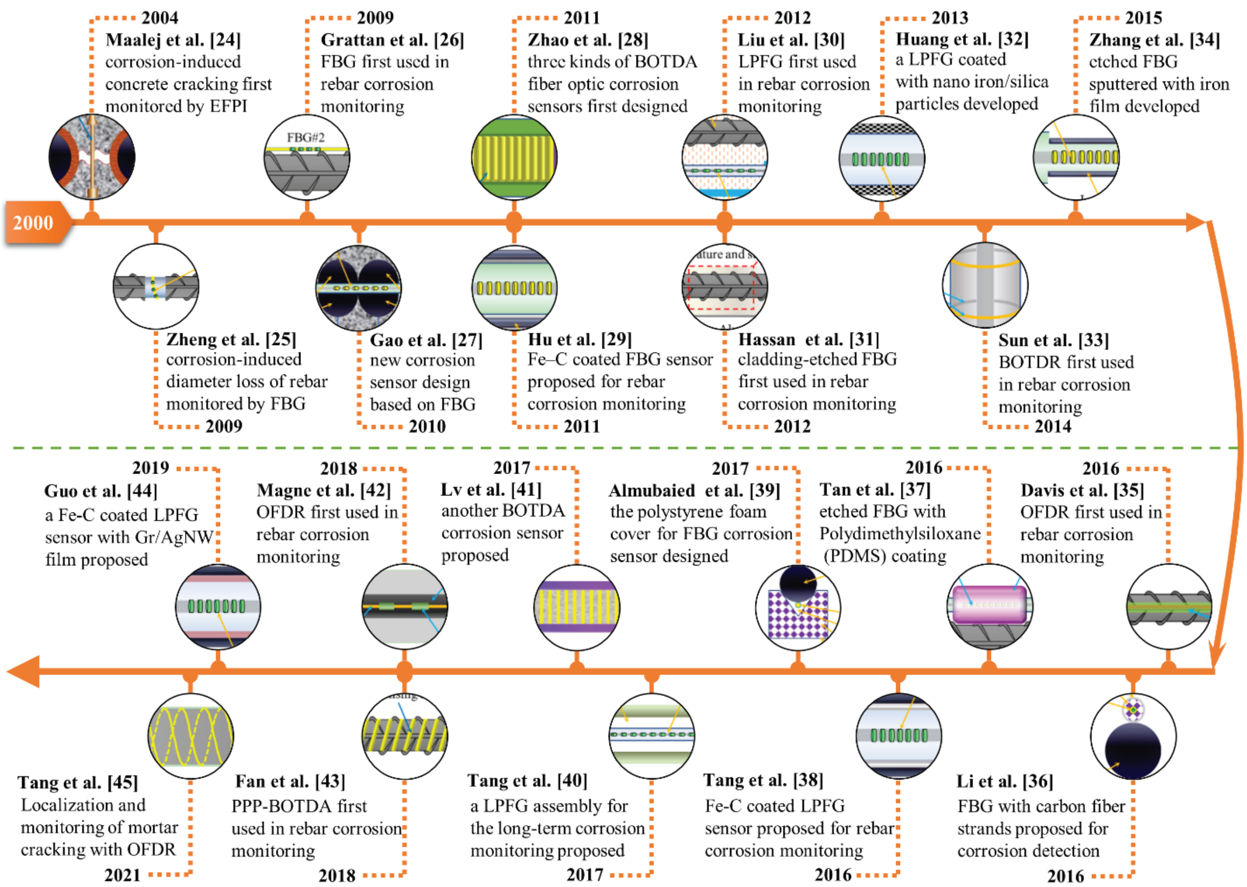

Fig. 1. Timeline of development of fiber optic sensors for corrosion monitoring of reinforcement steel in concrete [24-45].

3. Fiber Bragg grating fiber optic corrosion sensors

3.1 Sensing principle of FBG fiber

The fiber Bragg grating (FBG), also called short-period fiber grating, is a reflective band-pass filter component which is fabricated by periodically modifying the refractive index of the fiber core within a length of a few millimeters by using laser beam interference, photomask, or point-by-point method. As illustrated in Fig. 2, when a beam of broad spectral light is guided to pass through the Bragg gratings, some wavelengths that meet the Bragg condition shall be reflected back, and the others continue to travel through the grating region. The Bragg condition can be expressed as [46]

$$\lambda_B = 2n_{eff}\Lambda_B \tag{1}$$

where Λ_B is the spacing of Bragg grating (also known as the grating period) that is less than 1 μm, n_{eff} is the effective refractive index of the fiber core, and λ_B is the central wavelength of the reflected light which is called Bragg wavelength.

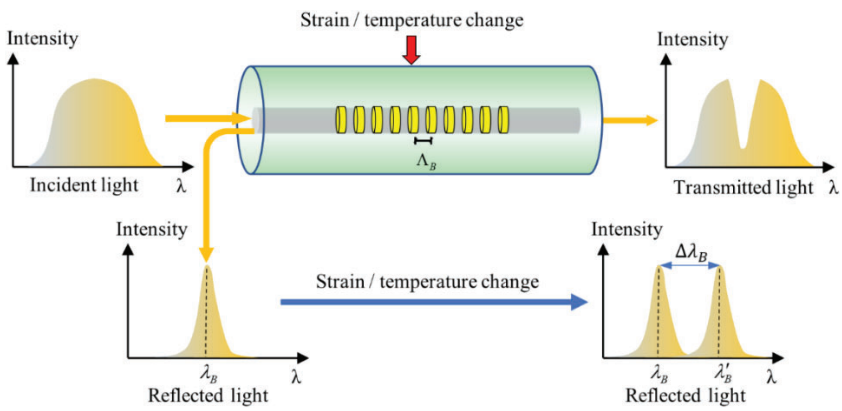

Fig. 2. Schematic illustration of the FBG sensing principle.

It can be inferred from Eq. (1) that the shift of Bragg wavelength arises due to either a change in the grating period or a change in the effective refractive index of the fiber core. The change of the grating period might be caused by elongation or compression of the fiber as it is attached on the surface of a tensioned or compressed structural component, and therefore it is widely employed for strain monitoring. In addition to the effect of fiber elongation, the effective core refractive index also changes due to strain-optic effect. Besides, the refractive index of the fiber core is dependent on the raw material that is used to fabricate the fiber core, and is affected by environmental factors such as temperature (called photo-elastic effect). As temperature changes, the spacing of Bragg grating changes due to thermal expansion (or contraction), and in the meantime the effective core refractive index changes due to thermo-optic effect. A general expression for the shift in Bragg wavelength due to temperature change considering the photon-elastic effect is given by [46-48]

$$\Delta\lambda_B = \varepsilon\left\{1-\frac{n_{eff}^2}{2}\left[p_{12}-\nu\left(p_{11}+p_{12}\right)\right]\right\}\lambda_B + \Delta T\left(\alpha_\Lambda+\alpha_n\right)\lambda_B \tag{2}$$

where ε is the applied strain, p_{11} and p_{12} are components of the strain-optic tensor, ν is the Poisson's ratio, ΔT is the temperature change, α_Λ is the thermal expansion coefficient of the fiber, α_n is the thermo-optic coefficient. Thus, the perturbation of external parameters can be sensed by analyzing the corresponding shift of Bragg wavelength taking into account possible thermo-optic effects.

3.2 FBG fiber optic corrosion sensors

FBG fiber optic corrosion sensors have the advantage that they require only a single-ended connection to the spectrometer as the reflected signal from the FBG is used for demodulation. In the following sections, the FBG fiber optic corrosion sensors will be categorized into three groups according to the deterioration process that is monitored: chemical reaction monitoring, steel bar corrosion monitoring and concrete expansion monitoring.

3.2.1 Chemical reaction monitoring

Corrosion-related chemical reaction monitoring in concrete structures with FBG optical fibers is realized by either directly monitoring the chemical reactions occurring around the fiber or monitoring the chemical reactions happening in a coating that is previously applied on the FBG fiber surface. For directly monitoring chemical reactions around the fiber, the cladding of the fiber needs to be removed first to expose the fiber core to the environment. A widely used method is chemical etching with concentrated nitric acid. Hassan et al. [31] used a cladding-etched FBG fiber sensor for temperature compensation during monitoring of steel bar corrosion in salt water. As shown in Fig. 3a, the fiber was first mounted on an aluminum plate to prevent fiber break during corrosion tests. As corrosion occurs in the steel rebar, the corrosion products change the environment around the cladding-etched FBG sensor and results in a shift of the reflected spectrum. Zhang et al. [34] sputter deposited a layer of iron film on a cladding-etched FBG fiber to monitor reinforcement steel corrosion. Corrosion of iron film changes the effective refractive index and consequently causes a shift of the reflected spectrum as schematically illustrated in Fig. 3b.

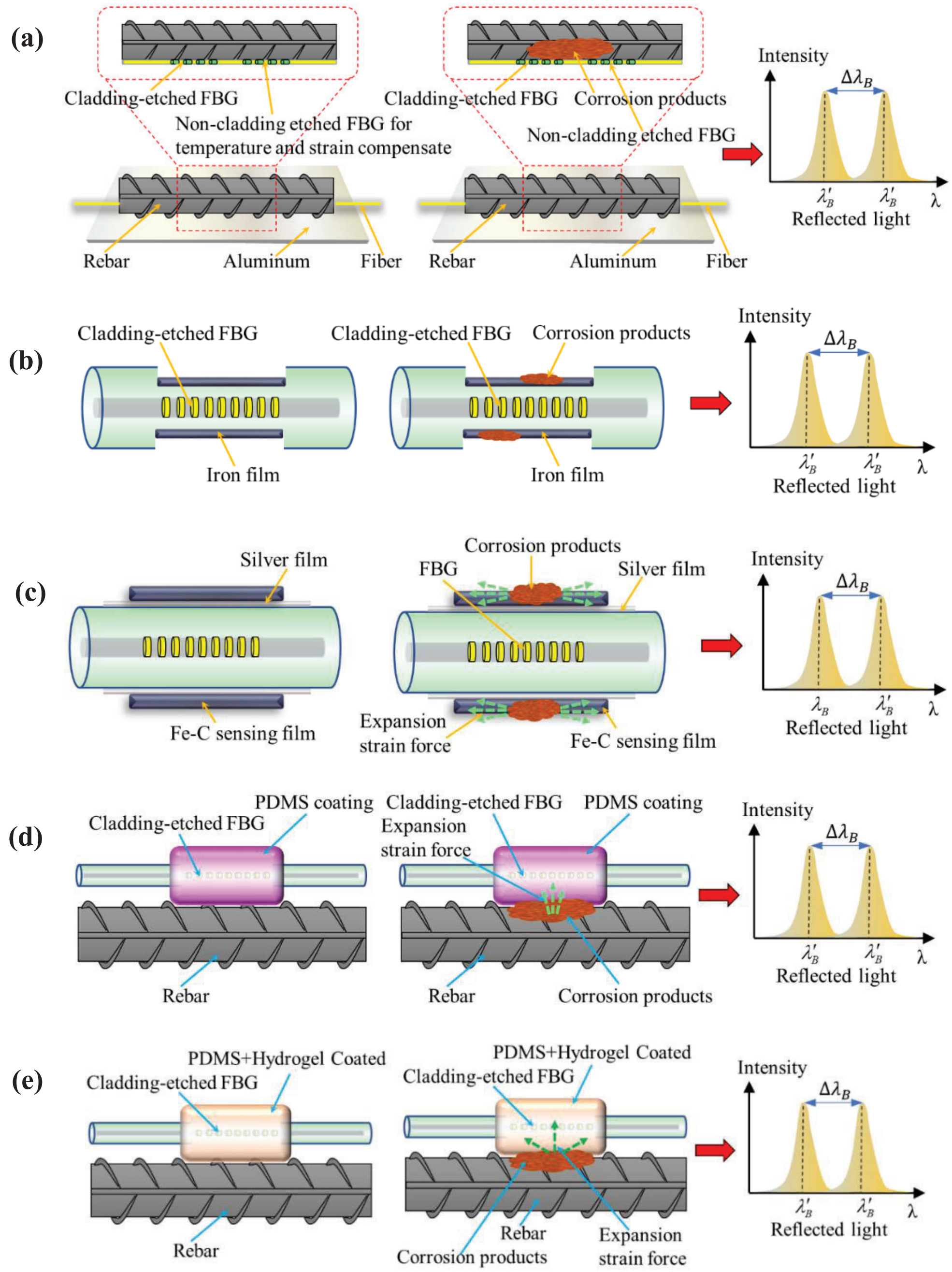

Fig. 3. Sensing principles of FBG fiber optic corrosion sensors based on corrosion-related chemical reactions: (a) cladding-etched FBG directly attached on the surface of steel rebars [31], (b) cladding-etched FBG coated with a layer of iron film [34], (c) FBG fiber coated with a layer of Fe-C film [29], (d) cladding-etched FBG coated with PDMS coating [37], and (e) cladding-etched FBG coated with a layer of PDMS and Hydrogel [49].

Hu et al. [29] proposed an Fe–C coated FBG sensor to monitor reinforcement steel corrosion as shown in Fig. 3c. A thin layer of silver was first sputter deposited to metalize the glass fiber, after which the Fe–C coating was electroplated on the grating region. As Fe-C coating corrodes, the expansive volume of corrosion products generates tensile stress in the fiber, which in turn is used to monitor steel corrosion. The Fe-C coated FBG fiber was experimentally investigated by direct immersion in NaCl solution. However, a relationship between the shift of the Bragg wavelength and the corrosion-induced mass loss of Fe-C coating could not be established. Moreover, the accuracy is significantly affected by the boundary conditions of the Fe-C coating as well as the mechanical properties of the corrosion products of the Fe-C coating.

A polydimethylsiloxane (PDMS) coating was applied on the fiber surface by Tan et al. [37] as shown in Fig. 3d, to increase the survival rate of the cladding-etched FBG optical fiber in the harsh environment of reinforced concrete structures. PDMS is a deformable and compliant material, which not only protects the FBG in the concrete but also acts as a media to transfer corrosion-induced expansion strain to the FBG fiber. Results showed that PDMS coated cladding-etched FBG fibers demonstrated a higher sensitivity for corrosion detection compared to non-coated fibers. Later, the PDMS coating was mixed with a pH-sensitive hydrogel as shown in Fig. 3e [49], and used to monitor steel corrosion at different environmental conditions namely air, acidic and alkaline environments. The major advantage of hydrogel is that it swells to varying degrees in different pH environments. When the pH values changes, the swelling rate of hydrogel changes, thus resulting in different expansion strain transferred to the FBG fiber through PDMS, and consequently leading to a shift in the Bragg wavelength.

3.2.2 Steel rebar corrosion monitoring

In the early phases of the corrosion propagation stage, corrosion products are formed which have a volume of 2-6 times greater than the original steel consumed. Therefore, some FBG fiber sensors are proposed that measure the corrosion-induced volume expansion of steel rebars.

By wrapping an FBG fiber around the polished surface of a steel rebar and attaching it with epoxy binder, Zheng et al. monitored corrosion-induced volume expansion of a steel rebar as shown in Fig. 4a [25, 50]. Through accelerated corrosion tests, a relation between the shift of the wavelength of the FBG fiber and the diameter loss of the steel rebar was established. Wrapping the FBG fiber around the corroding rebar might be beneficial in cases where the corrosion process is not uniformly distributed around the circumference of the steel rebar as is often observed in lab testing and practice. However, the measurement accuracy of this type of FBG sensor is also affected by the transverse stress of the fiber. Therefore, Chen and Dong theoretically studied the effects of transverse stress on the corrosion measurement accuracy of an FBG fiber sensor wrapped around a steel rebar [51]. An FBG based concrete package comprised of one FBG and twin rebar elements was proposed by Gao et al. as shown in Fig. 4b [27]. The steel rebar was first cut into two halves, and then a portion of the grating region of the FBG fiber went through and was fixed between them. As corrosion occurs, the volume of the twin steel bar increases and generates tensile stress in the fiber which can be recorded by an optical sensing instrument and used to monitor the corrosion of steel. This type of FBG fiber sensor only works for situations in which uniform corrosion occurs or localized corrosion happens between the twin rebars. In the case of localized corrosion occurance at other sides of the twin rebars, it will not work.

One advantage of FBG fiber sensors is the capability of being multiplexed into a network for distributed sensing. By connecting a few FBG sensors in series and attaching them on the surface of a steel rebar as shown in Fig. 4c, Grattan et al. [26, 52] found that the FBG-based sensor system was able to monitor localized corrosion in steel rebars by detecting the changes in strain. The monitoring accuracy of this type of sensor arrangement that is parallel to the length of a steel rebar is affected by the stress levels in the steel rebars.

Most FBG fibers are made of brittle glass silica and therefore, some protection measures have to be taken when deployed in concrete structures. Almubaied et al. [39] proposed and investigated an FBG sensor mounting technique. As shown in Fig. 4d, the FBG fiber sensor was first fixed on the surface of steel rebars by using epoxy, and then covered with a V-shape cut polystyrene foam. On one hand, the polystyrene foam allows the water to go through it to reach the steel rebar surface and cause corrosion. On the other hand, the foam possesses good energy absorption and deformability that would protect the FBG fibers from damage during concrete pouring and compaction. However, it should be noted that the presence of polystyrene foam might hinder the stress transfer between reinforcement steel and concrete, and hence should be considered carefully in highly stressed zones of structural elements.

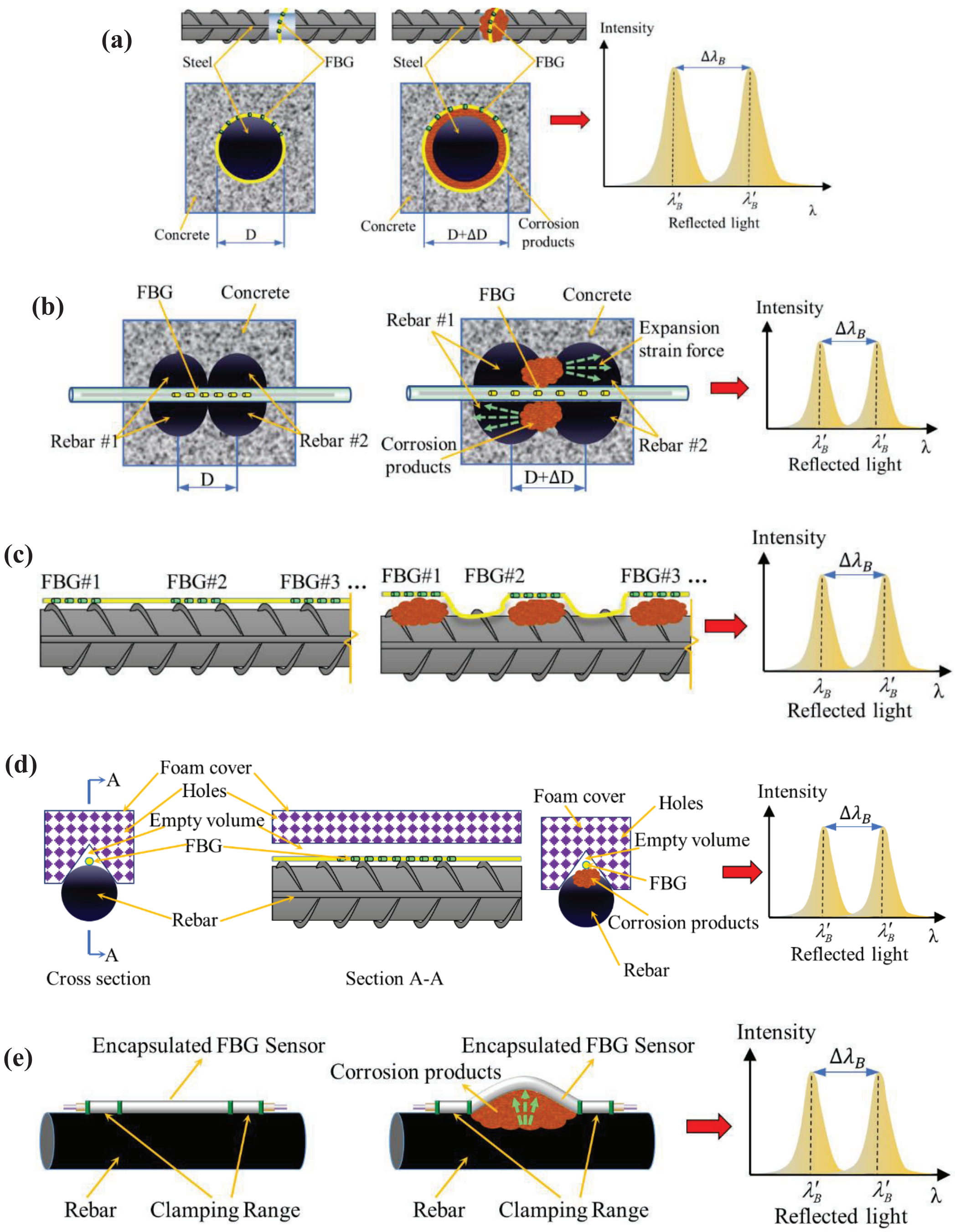

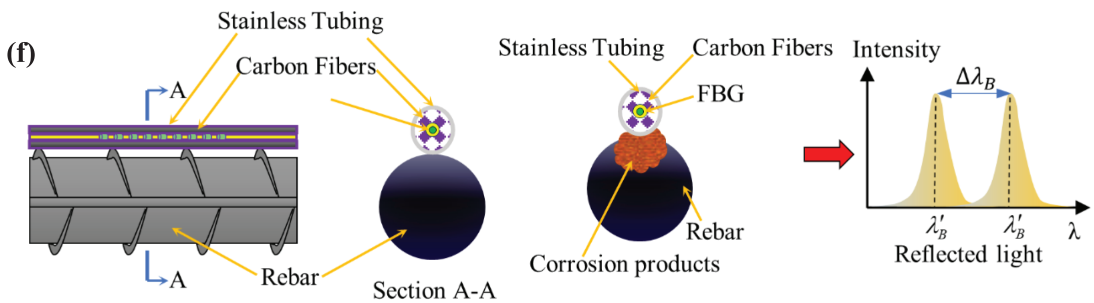

Fig. 4. Sensing principle of FBG fiber optic corrosion sensors by monitoring steel rebar corrosion: (a) FBG optical fiber directly wrapped on the surface of a steel rebar [25], (b) FBG optical fiber embedded in twin steel rebars [27], (c) FBG optical fiber periodically attached on the surface of a steel rebar [26], (d) FBG optical fiber placed in a precut foam covered along the length of a steel rebar [39], (e) FBG fiber encapsulated in a stainless steel tube and clamped on the surface of a steel rebar [53], (f) FBG fiber encased in stainless steel tube with carbon fibers and attached on the surface of a steel rebar [36].

By encapsulating an FBG fiber in a stainless steel tube and attaching it on the surface of a steel rebar with the two ends fixed as shown in Fig. 4e, Sun et al. studied the performance of FBG fibers for corrosion monitoring of reinforcement steel through accelerated corrosion tests [70]. As corrosion occurs in the steel rebar, the expansive corrosion products exert pressure against the stainless steel tube and cause deformation of the tube and subsequently a shift of Bragg wavelength. This FBG corrosion sensor has a low monitoring sensitivity, as it is significantly affected by the thickness and mechanical properties of the stainless steel tube, the stress transfer ratio between the stainless steel tube and the FBG fiber inside, and the expansive stress level of the corrosion products. Moreover, it is not suitable for monitoring localized corrosion that occurs away from the stainless steel tube.

In addition to monitoring volume expansion of corroded steel rebars, FBG fiber sensors were also proposed that operate by monitoring inhibition of heat transfer of corrosion products. The thermal conductivity of corrosion products is lower than that of steel and concrete, and therefore they inhibit transfer of heat. Based on this phenomenon, an FBG fiber sensor combined with carbon fiber strands and an active thermal probe was proposed for corrosion detection as shown in Fig. 4f [36]. Both the FBG fiber and carbon fiber strands were encapsulated in a thin-walled stainless steel tube that was mounted on the surface of a steel bar as a heat source. The FBG fiber serves as a temperature sensor of the heat source, and an active thermal probe which is placed at the steel-concrete interface is used to detect the thermal transfer through the corrosion product layer. When the steel corrosion proceeds, the time-response of the temperature detected by the active thermal probe changes as a result of the reduced thermal conductivity of corrosion products. Therefore, after injecting heat through carbon fiber strands, the steel corrosion degree can be detected based on temperature response measured by the active thermal probe. It should be noted that the FBG fiber of this corrosion monitoring assembly only works as a temperature sensor of the heat source, and the correlation between the time response of the thermal probe and the corrosion-induced mass loss of steel rebar was is not yet fully understood [36]. Moreover, this corrosion sensor is only suitable for uniform corrosion monitoring or localized corrosion that occurs around the stainless steel tube.

3.2.3 Concrete expansion monitoring

In later phases of the corrosion propagation stage, more and more corrosion products are produced and exert expansive pressure against the surrounding concrete, causing concrete cracking and spalling. Therefore, FBG based sensors for rebar corrosion monitoring in this stage are also proposed by measuring corrosion-induced concrete cover expansion or cracking.

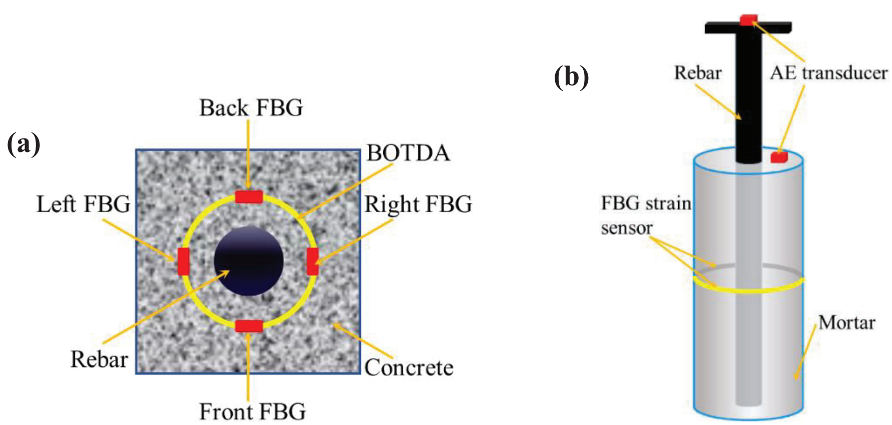

Fig. 5. FBG optic fiber corrosion sensors based on concrete expansion: (a) four FBG fiber sensors uniformly distributed around the concrete surrounding a steel rebar [54], and (b) one FBG fiber attached on the surface of a concrete cylinder containing a steel rebar in the core [55].

By wrapping distributed FBG fibers around the concrete surrounding the steel rebar as shown in Fig. 5a, Mao et al. found that FBG fibers could not only identify the crack initiation time and but also the position of corrosion induced concrete cracking as shown in Fig. 5a [54]. Li et al. also investigated corrosion-induced concrete cracking by using combined acoustic emission sensors and an FBG fiber attached on the concrete surface as shown in Fig. 5b [55]. The drawback of this type of fiber installation is that the monitoring accuracy is significantly affected by the properties of the concrete cover.

3.3 Performance of FBG corrosion sensors

In the literature, indoor lab tests are conducted to study the feasibility of these sensors for corrosion monitoring. However, the majority of these studies did not discuss the performance parameters of the sensors proposed. In this section, the performance parameters of these FBG fiber optic corrosion sensors mentioned above will be discussed in detail, including the measurand, sensitivity, monitoring range and service life. The factors affecting these parameters are summarized in Table 1 and Table 2.

For cladding-etched FBG fiber optic corrosion sensors as shown Fig. 3a, the fiber monitors steel rebar corrosion through sensing the accumulation of corrosion products surrounding the fiber. Therefore, the measurand is the refractive index and the sensitivity is dependent on the diffusion rate of corrosion products from the rebar surface to the fiber, and is affected by the distance between them. Moreover, the sensitivity might decrease with an increase of corrosion time, since the fiber is less sensitive to the accumulation of the corrosion products further away from the fiber. Based on the test results, the total shift of the Bragg wavelength is around 1 nm after 74 days immersion in salt solution [31]. However, the total range of the Bragg wavelength shift was not yet obtained as the corrosion test terminated after 74 days. The service life of this FBG fiber corrosion sensor is dependent on the corrosion rate of the steel rebar and it could potentially survive the entire service life of the structure.

For cladding-etched iron coated FBG corrosion sensors as shown in Fig. 3b, a 30 nm thick iron film was sputter coated on the etched FGB fiber, and a rate of 0.05 nm per hour was observed in Bragg wavelength shift during a corrosion test in 3.5 wt.% NaCl solution [34]. Although the effect of iron film thickness on the monitoring sensitivity was not investigated, the sensitivity of this FBG corrosion sensor is dependent on the porosity and thickness of the sputter iron film. The corrosion test was terminated after 10 hours of immersion in salt solution with a total shift of 0.5 nm in Bragg wavelength [34]. For steel rebar corrosion monitoring, the monitoring range in terms of corrosion-induced mass loss will be dependent on the ratio of the volume of iron film to the steel rebar. The service life is dependent on the thickness and corrosion rate of the iron film, and a service life of only 10 hours was observed with a 30 nm thick iron film for corrosion monitoring in 3.5 wt.% NaCl solution [34].

For Fe-C coated FBG optic fiber corrosion sensor as shown in Fig. 3c, the sensitivity is dependent on the mechanical properties of fiber glass, Fe-C film and corrosion products, as well as the bond strength between fiber and Fe-C film. Regarding the monitoring range in terms of Bragg wavelength shift, an average shift of 0.051 nm was observed in 0.5 mol/L NaCl solution, and 0.625 nm shift was obtained embedded in sponge that was partially immersed in NaCl solution [29]. For monitoring range in terms of corrosion loss, it depends on the ratio of the volume of Fe-C film to the steel rebar. The service life is primarily dependent on the thickness and corrosion rate of Fe-C film, and it may range from a few to tens of days. A service life of around 80 days and 40 days was observed for 12-15 μm thick Fe-C film when immersed in 0.5 mol/L NaCl solution and embedded in sponge that was partially immersed in salt solution, respectively [29].

For PDMS coated FBG fiber sensor as shown in Fig. 3d, the measurand is strain. The sensitivity is dependent on the mechanical properties and thickness of PDMS coating, the bond strength between fiber and PDMS coating, and the diameter of FBG fiber. PDMS coated fully-etched FBG fiber demonstrated a higher sensitivity than that without chemical etching, and a Bragg wavelength shift less than 0.01 nm was observed after 60 days immersion in a solution with pH 4.0 [37]. The service life is primarily dependent on the durability of PDMS coating and corrosion rate of steel rebar, and it might survive the entire service life of structures if the PDMS coating does not age in concrete.

For FBG fiber sensors coated with PDMS and hydrogel as shown in Fig. 3e, the measurand is also strain. In addition to the factors similar to PDMS coated fiber sensor, the content of hydrogels, pH values and ionic concentration of the environment also affect the monitoring sensitivity. The monitoring range is dependent on the content of hydrogels, pH values and ionic concentration of the environment. The service life is primarily dependent on the durability of PDMS and hydrogel coating, the environment, and the corrosion rate of steel rebars.

Table 1. Factors affecting the performance of FBG fiber optic corrosion sensors based on chemical reaction monitoring.

Sensor	Measurand	Sensitivity	Experimentally observed monitoring range	Service life
Fig.3a [31]	Refractive index	Affected by the distance between the fiber and the steel rebar, and the diffusion rate of corrosion products toward the fiber.	Around 1.0 nm in Bragg wavelength shift after 74 days immersion in salt solution.	Depends on the corrosion rate of steel rebars, can potentially survive the entire service life of structures if properly protected.
Fig.3b [34]	Refractive index	Primarily depends on the porosity and thickness of sputter coated iron film.	Depends on the thickness of iron film, around 0.5 nm Bragg wavelength shift for 30 nm thick iron film. For steel rebar corrosion monitoring, it depends on the ratio of the volume of iron film to the steel rebar.	Depends on the thickness and corrosion rate of iron film, ranging from a few to tens of hours. Around 10 hours in 3.5 wt.% NaCl solution with 30 nm thick iron film.
Fig.3c [29]	Strain	Depends on the mechanical properties of fiber glass, Fe-C coating and corrosion products, as well as the bond strength between Fe-C coating and fiber.	For 12-15 μm thick Fe-C film, a resonant wavelength shift of 0.051 nm in 0.5 mol/L NaCl solution, and 0.625 nm shift when embedded in sponge that is partially immersed in NaCl solution. For steel rebar corrosion monitoring, it depends on the ratio of the volume of Fe-C film to the steel rebar.	Depends on the thickness and corrosion rate of Fe-C film, ranging from a few to tens of days in slat solution. Around 80 days in 0.5 mol/L NaCl solution with 12-15 μm thick Fe-C film.
Fig.3d [37]	Strain	Depends on the thickness and mechanical properties of PDMS coating, interfacial bond between PDMS coating and fiber, and the FBG fiber diameter.	A Bragg wavelength shift less than 0.01 nm was observed after 60 days immersion in a solution with pH 4.0.	Depends on the durability of PDMS coating and corrosion rate of steel rebar.
Fig.3e [49]	Strain	Depends on the thickness and mechanical properties of PDMS coating, interfacial bond between PDMS coating and fiber, the FBG fiber diameter, content of hydrogels, pH values and ionic concentration of the environment.	A Bragg wavelength shift of 1.8 nm, 1.0 nm and 0.2 nm was observed in acidic, air and alkaline conditions, respectively.	Depends on the durability and stability of PDMS and hydrogel coating, the pH values and ionic concentration of the environment, and corrosion rate of steel rebar.

The FBG fiber optic corrosion sensors coated with a layer of iron film, Fe-C film, PDMS coating or PDMS coating with hydrogel show a higher sensitivity and are capable of detecting corrosion at a very early stage. However, their sensitivity will decrease significantly in later stage as the iron film or Fe-C film is completely corroded [34] or the PDMS coating is chemically stabilized [56, 67]. Therefore, they are suitable for corrosion monitoring in initiation stage.

Table 2. Factors affecting the performance of FBG fiber optic corrosion sensors based on steel bar corrosion and concrete expansion monitoring.

Sensor	Measurand	Sensitivity	Monitoring range	Service life
Fig. 4a [25] and Fig.4b [27]	Strain	The sensitivity is primarily dependent on the wrap tightness of the fiber, expansion ratio and mechanical properties of corrosion products.	Primarily depends on the wrap tightness of the fiber, expansion ratio and mechanical properties of corrosion products, and demodulation technique.	Mainly depends on the corrosion rate of steel rebar, and might survive the entire service life of structures if protected properly.
Fig. 4c [26] and Fig.4d [39]	Strain	Depends on the volume expansion ratio and mechanical properties of corrosion products.	Depends on the mechanical property of fiber glass and the demodulation technique	Primarily depends on the corrosion rate of steel rebar, and might survive the entire service life of structures if protected properly.
Fig. 4e [53]	Strain	Depends on the thickness and mechanical properties of the stainless steel tube, the stress transfer ratio between the stainless steel tube and the FBG fiber inside, and the expansive stress level of the corrosion products	Depends on the volume expansion ratio of corrosion products, clamped length of stainless steel tube, diameter of steel rebar, and demodulation technique.	Depends on the corrosion rate of steel rebar and might survive the entire service life of structures if protected properly.
Fig. 4f [36]	Temperature	Depends on the thermal conductivity of materials surrounding the probe, such as mortar layer, stainless steel tube and corrosion products	Theoretically can monitor corrosion loss of steel rebar up to 100%.	Depends on the corrosion rate of steel rebar and might survive the entire service life of structures if protected properly.
Fig.5a [54] and Fig.5b [55]	Strain	Depends on the thickness and properties of concrete cover, the properties of corrosion products, wrap tightness of FBG fiber, and mechanical properties of epoxy resin.	Depends on the maximum elongation of FBG fiber and the corresponding demodulation capacity of the instrument, and is affected by the mechanical properties and durability of epoxy resin.	Depends on the corrosion rate of steel rebar, is affected by the durability of epoxy resin and other mechanical cracks. It might survive the entire service life of structures if protected properly.

For an FBG fiber that is wrapped around the surface of a steel rebar (Fig. 4a) or goes through a parallel twin steel rebar (Fig. 4b) to monitor steel rebar corrosion as shown in Table 2, the sensitivity of corrosion monitoring is dependent on the tightness of the wrapped fiber or embedded fiber inside the twin rebars as well as the expansion ratio and mechanical properties of corrosion products. The relationship between the corrosion-induced strain in the fiber and the corrosion mass loss of a steel rebar can be expressed as:

$$\eta = 1-(1-\frac{\varepsilon}{k-1})^2 \tag{3}$$

where η is the corrosion-induced mass loss of steel rebar, k is the volume expansion ratio of corrosion products, and ε is corrosion-induced strain in the FBG fiber. A typical FBG fiber can measure strain as high as 10000 με, and assuming an expansion ratio k=2~6, based on Eq. (3) the monitoring range in terms of mass loss of the steel rebar can be calculated to range from 0.4% to 2.0%. In practice, the corrosion products might be squeezed out beneath the wrapped fiber, and therefore the monitoring range in terms of mass loss of the steel rebar would be higher than the theoretical values. The service life of this FBG sensor is primarily dependent on the corrosion rate of the steel rebar.

For FBG fiber corrosion sensors as shown in Fig. 4e, the sensitivity is dependent on the thickness and mechanical properties of the stainless steel tube, the stress transfer ratio between the stainless steel tube and the FBG fiber inside, and the expansive stress level of the corrosion products against the stainless steel tube. Assuming the corrosion-induced deformation of the stainless steel tube is linear and satisfying with the Pythagorean theorem [53], the relationship between the corrosion-induced mass loss of steel rebar η and the strain in the FBG fiber ε is:

$$\eta = \frac{1}{k-1}[(1+\frac{L}{D}\sqrt{\frac{\varepsilon}{2}})^2-1] \tag{4}$$

where k is the volume expansion ratio of corrosion products, L is the clamped length of the stainless steel tube along the length of the steel rebar, and D is the diameter of the steel rebar. Assuming L=50 mm, D=20 mm, k=3, the theoretical mass loss of the steel rebar η is calculated to be 19 wt. % as the fiber strain is 10000 με. In practical application, the monitoring range regarding corrosion-induced mass loss of the steel rebar might be higher than the theoretical value, as some corrosion products will diffuse out and the corrosion-induced deformation of the stainless steel tube is not fully transferred to the FBG fiber inside. The service life of this FBG fiber optic corrosion sensor is dependent on the corrosion rate of the steel rebar and the sensor can potentially survive the entire service life of structures if protected properly.

For steel rebar corrosion monitoring with FBG fibers encased in a stainless steel tube with carbon fibers as show in Fig. 4f, the corrosion monitoring sensitivity is dependent on the thermal conductivity of the materials surrounding the probe, such as mortar layer, stainless steel tube and corrosion products. This carbon fiber/FBG active thermal probe can monitor corrosion loss of a steel rebar (theoretically) up to 100%. A maximum 5.72% mass loss was experimentally obtained and reported in the literature [36]. Again, the service life of this corrosion probe could potentially survive the entire service life of the RC structure.

For FBG fiber optic corrosion sensors wrapped in or around the concrete cover with epoxy resin as shown in Figs. 5a and 5b, both the sensitivity and monitoring range are dependent on the thickness and properties of the concrete cover (tensile strength, porosity and elastic modulus), the properties of corrosion products (volume expansion, elastic modulus), mechanical properties of epoxy resin, and wrap tightness of the FBG fiber. The service life is primarily dependent on the corrosion rate of the steel rebar, and is also affected by the thickness and properties of the concrete cover, the elastic strain capacity of the FBG fiber, and the durability of epoxy resin.

To sum up, for these sensors based on the measurement of corrosion-induced volume expansion of steel rebars and concrete, the sensitivity is highly dependent on the packaging technique or installation method, the mechanical properties of corrosion products, and the thickness and material properties of surrounding concrete. The monitoring range is primarily dependent on the capacity of the instruments or the demodulation technique. The service life, when counted from the start of the corrosion process, is mainly dependent on the corrosion rate of the steel rebar, and is also affected by the capacity of the instrument or the demodulation technique, while the whole lifetime of the sensor also depends on the durability of the packaging materials.

4. Long period fiber grating-based corrosion sensors

4.1 Sensing principle of LPFG

Different from FBG, LPFG is a transmitted band-rejection filter component with a typical grating period ranging from 100 μm to 1 mm [56]. As illustrated in Fig. 6, as a beam of broadband spectral light is guided to pass through the LPFG inscribed in a single mode fiber, light traveling in the core mode will couple with light co-propagating in the cladding modes, resulting in a series of attenuation bands in the transmitted spectrum at specific wavelengths that meet the phase-matching condition, and the central wavelength of the attenuation bands is the resonant wavelength which can be expressed by [56]

$$\lambda_{res,m} = (n_{eff}^{co} - n_{eff}^{cl,m})\Lambda \tag{5}$$

where Λ is the grating period, n_{eff}^{co} is the effective refractive index of core mode which is associated with the core refractive index n_1 and the cladding refractive index n_2, $n_{eff}^{cl,m}$ is the effective refractive index of m-th cladding mode that is dependent on n_1, n_2 and the surrounding environmental refractive index n_{sur}, and $\lambda_{res,m}$ is the resonant wavelength corresponding to m-th cladding mode.

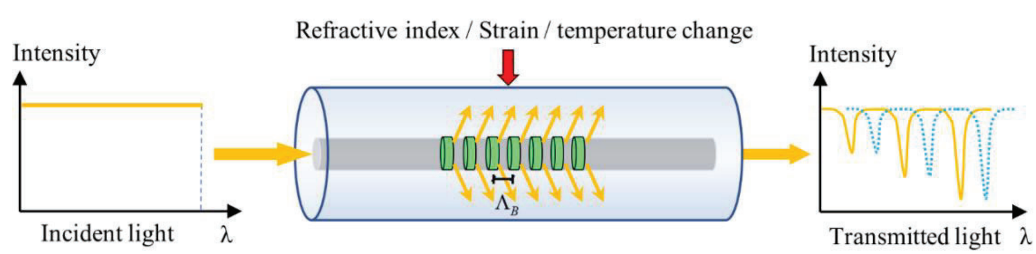

Fig. 6. Schematic illustration of the LPFG sensing principle.

It can be inferred from Eq. (5) that the shift of the resonant wavelength happens as the grating period changes and/or a change occurs for the effective refractive index of the core mode and cladding mode $(n_{eff}^{co} - n_{eff}^{cl,m})$, which might be induced by external disturbance such as strain, temperature, the substances surrounding the fiber, etc. [57]. Therefore, by observing the shift of the resonant wavelength, the change of these external parameters can be detected.

4.2 LPFG fiber optic corrosion sensors

A number of LPFG based sensors have been proposed and investigated for steel corrosion monitoring over the past decade. Liu et al. [30]reported an LPFG based sensor for monitoring reinforcement steel corrosion in concrete as shown in Fig. 7a. The sensor consists of a stainless-steel base that was fully filled with phenolic resin and a bare LPFG fiber merged in the phenolic resin. As steel corrodes, corrosion products dissolve into the phenolic resin and subsequently change the refractive index of environment surrounding the LPFG fiber, resulting in a change of the effective refractive index. Thus, a real-time monitoring of steel corrosion condition can be achieved by analyzing the resonant wavelength shift.

By dispersing nano iron/silica particles in polyurethane and then applying on the surface of an LPFG fiber, Huang et al. [32, 58] proposed an LPFG sensor for steel rebar corrosion monitoring as shown in Fig. 7b. Since the nano iron particles have similar chemical composition as the steel rebar, the effective environmental refractive index will change as iron particles corrode, and consequently causes a shift in the resonant wavelength, which in turn is used for corrosion monitoring. Later on, Fe-C coated LPFG sensors were proposed for steel rebar corrosion monitoring in reinforced concrete structures as shown in Figs. 7c [38, 59, 60]. When the Fe-C coating gradually corrodes and corrosion products are generated, the surrounding environmental refractive index around the LPFG changes accordingly, resulting in a shift of the resonant wavelength. By establishing a relationship between the corrosion-induced mass loss of Fe-C coating and the shift of the resonant wavelength, Fe-C coated LPFG fiber sensors can be used to monitor initiation of steel reinforcement corrosion. The fiber used was made of glass silica and not conductive, therefore a thin layer of silver film was first deposited before electroplating the outer Fe-C coating layer. The sensitivity, effective monitoring range and service life of these Fe-C coated LPFG fiber corrosion sensors were characterized in 3.5wt.% NaCl solution and simulation concrete pore solutions [61, 62]. The Fe-C coated LPFG sensor was also employed to monitor growth of passive film on a steel rebar in saturated concrete pore solution as shown in Fig. 7d [63]. To increase the sensitivity, the inner silver layer was replaced with a graphene/silver nanowire (Gr/AgNW) film as shown in Fig. 7e [44, 64]. Theses Fe-C coated LPFG corrosion sensors have the same monitoring principle, but with different service life, sensitivity, and monitoring range depending on the type and thickness of both inner conductive film and the outer Fe-C coating.

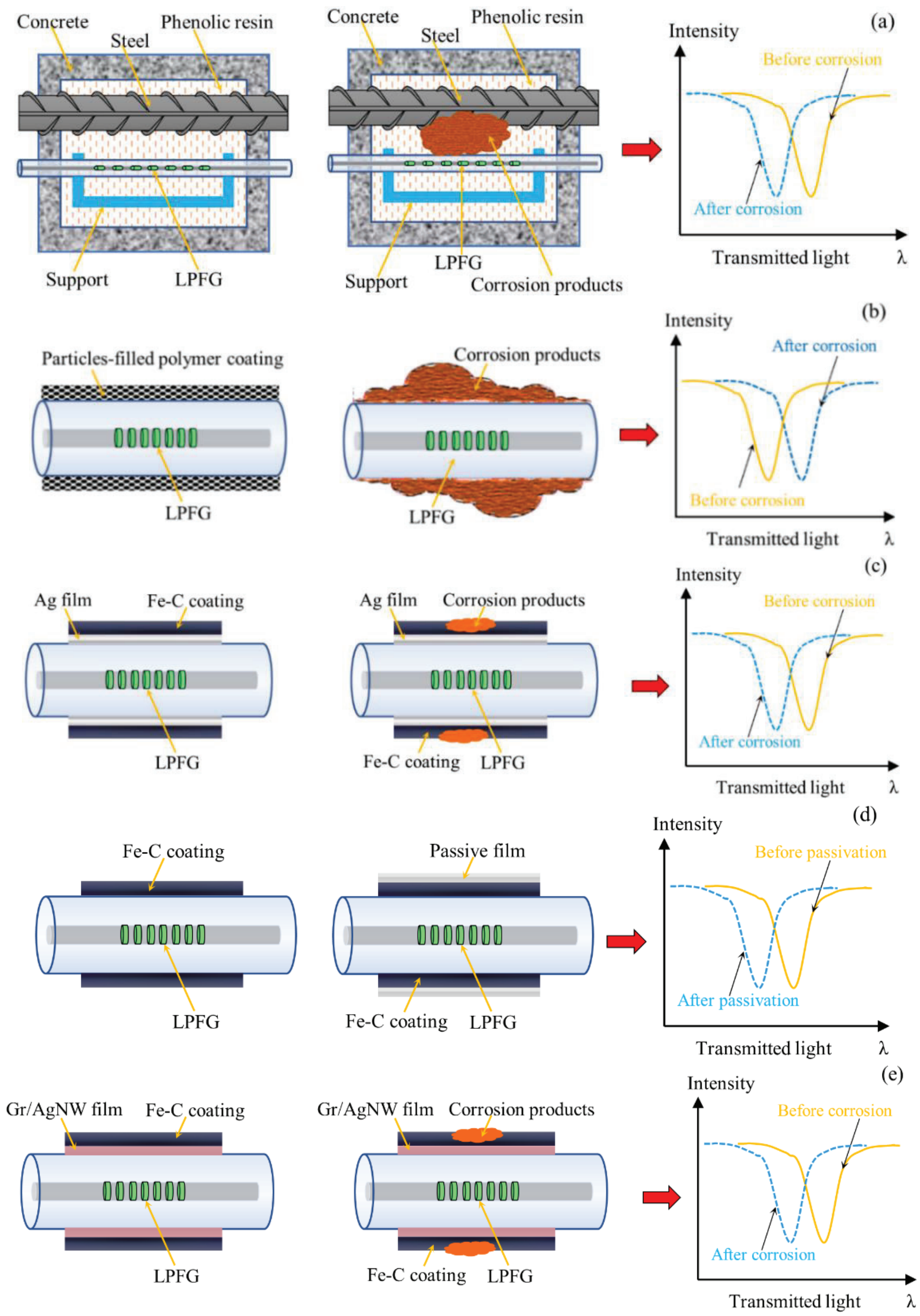

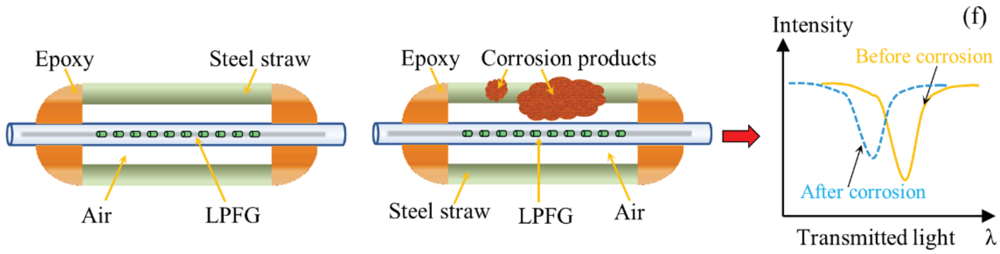

Fig. 7. Sensing principle of various LPFG corrosion sensors: (a) bare LPFG fiber merged in phenolic resin [30], (b) LPFG fiber coated with nanoparticle-filled polymer [32], (c) Fe-C coated LPFG for steel corrosion monitoring [59], (d) Fe-C coated LPFG for steel passivation monitoring [63], (e) Gr/AgNW and Fe-C coated LPFG [64], (f) LPFG fiber encased inside a steel straw [40].

These Fe-C coated LPFG corrosion sensors mentioned above have short service lives that range from a few hours to a few days since the thickness of Fe-C coating is in the order of micrometer. For RC structures, the designed service life can reach 120 years. Therefore, these Fe-C coated corrosion sensors are not suitable for long-term corrosion monitoring of RC structures. To increase the service life, Tang et al. [40] proposed a LPFG assembly for long-term corrosion monitoring of reinforcement steel in concrete as shown in Fig. 7f. The assembly was comprised of a steel straw made of the same material as the steel bar but with different wall thickness. One LPFG fiber passes through the inner cavity of the steel straw until the grating region is completely encased inside the steel straw, and then the two ends of the steel straw are sealed by using Epoxy. Initially the surrounding environment around the grating region is air, and gradually it becomes a mixture of corrosion products, water and other chemicals as corrosion penetrates the wall of the steel straw, and consequently results in a shift of the resonant wavelength. The time of the shift of the resonant wavelength corresponds to a corrosion penetration depth that equals the wall thickness of the steel straw. With different wall thicknesses, the LPFG assembly can be deployed in concrete for long-term corrosion monitoring.

4.3 Performance of LPFG corrosion sensors

The parameters of LPFG fiber optic corrosion sensors mentioned in section 4.2 are summarized in Table 3, including the measurand, sensitivity, monitoring range and service life. Since all LPFG fiber optic corrosion sensors as mentioned above are based on the change of the effective environmental refractive index, the measurand is the refractive index. For bare LPFG in phenolic resin as shown in Fig. 7a, the sensitivity is dependent on the distance between the LPFG fiber and the steel rebar, the porosity of the phenolic resin, and the diffusion coefficient of corrosion products in phenolic resin. From experimental tests, it was reported that the resonant wavelength blue shifted 9.327 nm in the first 65 days, then red shifted 10.174 nm from 66 to 112 days, and became stabilized after 112 days for a 25 mm-diameter steel rebar subjected to accelerated corrosion tests. The total corrosion-induced mass loss after 112 days was equivalent to approximately 10 years for a steel rebar under natural corrosion [30]. Therefore, the effective monitoring range is 10.174 nm in terms of resonant wavelength shift and approximately 20% in terms of mass loss of the steel rebar. The service life is dependent on the actual corrosion rate of the steel rebar and is around 10 years based on the prediction reported in [30].

For LPFG fibers coated with a layer of nano iron/silica particle filled polyurethane as shown in Fig. 7b, the sensitivity is dependent on the thickness and porosity of nanoparticle-filled polyurethane, and it decreases with an increase of corrosion time. It was reported in [32] that the resonant wavelength red shifted around 0.50 nm after 800 hours of immersion in 3.5% NaCl solution, after which it gradually stabilized. Therefore, the monitoring range is around 0.5 nm in terms of the resonant wavelength shift, and the corresponding mass loss and service life are dependent on the corrosion rate and the total mass of the nano iron particles dispersed in the polyurethane coating.

For Fe-C coated LPFG fiber corrosion sensors as shown in Figs. 7c, 7d, and 7e, the sensitivity is dependent on the thickness and porosity of both inner silver or Gr/AgNW film and outer Fe-C coatings. The monitoring range and service life are dependent on the thickness of the Fe-C coating. It should be noted that these parameters are based on the mass loss of the outer iron or Fe-C coating which is previously deposited on the fiber. These metal films are nano-structured and have different chemical compositions than steel reinforcement. Therefore, their corrosion rate is different from that of the steel rebar. In addition, as discussed in the previous section, the LPFG fiber optic corrosion sensors have very limited service life that ranges from a few hours to a few days, which makes them rather unsuitable for long-term corrosion monitoring. The advantage of these LPFG fiber optic corrosion sensors is that they are very sensitive to environmental changes and therefore, are suitable for monitoring corrosion initiation of steel bars in concrete. For LPFG fibers encased in a steel straw as shown in Fig. 7f, the sensitivity, monitoring range and service life are all dependent on the wall thickness of steel straw, and the service life is also affected by the corrosion rate of the steel straw.

Table 3. Factors affecting the performance of LPFG fiber optic corrosion sensor.

Sensor	Measurand	Sensitivity	Experimentally observed monitoring range	Service life
Fig.7a [30]	Refractive index	Depends on the distance between the LPFG fiber and steel rebar, the porosity and diffusion coefficient of corrosion product in phenolic resin.	Up to 20% corrosion-induced steel mass loss.	Depends on the corrosion rate of steel rebar. Approximately a service life of 10 years.
Fig.7b [32]	Refractive index	Depends on the thickness and porosity of nanoparticle-filled polyurethane coating, decreases with an increase of corrosion time.	Can monitor up to 100% corrosion of nano iron particles; for steel rebar, it depends on the mass ratio of nano iron particle to steel rebar.	Depends on the total mass and corrosion rate of iron particles in polyurethane coating.
Fig.7c [59]	Refractive index	Depends on the thickness and porosity of both inner silver film and outer Fe-C coating, 0.06~0.22 nm/1% Fe-C mass loss in 3.5 NaCl solution.	Up to 95.2% Fe-C mass loss; For corrosion monitoring of steel rebar, it depends on the mass ratio of Fe-C coating to steel rebar.	Depends on the thickness and corrosion rate of Fe-C coating.
Fig.7d [63]	Refractive index	Depends on the thickness and porosity of both inner silver film and outer Fe-C coating, 0.17~0.25 nm/0.01 nm thick passive film growth in saturated $Ca(OH)_2$ solution.	Up to 0.60 nm thick of passive film.	Depends on the thickness and passivation rate of Fe-C coating.
Fig.7e [64]	Refractive index	Depends on the thickness and porosity of both inner Gr/AgNW film and outer Fe-C coating, 0.091~0.346 nm/1% Fe-C mass loss in 3.5 % NaCl solution.	Up to 95% Fe-C mass loss, For corrosion monitoring of steel rebar, it depends on the mass ratio of Fe-C coating to steel rebar.	Depends on the thickness and corrosion rate of Fe-C coating.
Fig. 7f [40]	Refractive index	Depends on the wall thickness of steel straw. The thinner the wall, the higher the sensitivity.	Depends on the wall thickness of steel straw. For corrosion monitoring of steel rebar, it depends on the ratio of wall thickness to steel rebar diameter.	Depends on the corrosion rate and wall thickness of steel straw.

5. Extrinsic Fabry-Perot interferometer-based corrosion sensors

5.1 Sensing principle of EFPI

The extrinsic Fabry-Perot interferometer (EFPI) typically consists of a lead-in fiber and a component with a reflecting/mirror-like surface, as illustrated in Fig. 8. The lead-in fiber end-face is separated from the reflecting surface of the component by an air gap, called the Fabry-Perot cavity [65-67]. As the incident light travels in the lead-in fiber, the first reflection occurs at the interface between the lead-in fiber and the air in the gap, and the remaining light continues to travel through the Fabry-Perot cavity. The second reflection occurs at the interface between the cavity and the reflecting surface of the component. These two reflected light beams interfere and produce an interference pattern. A general expression for the intensity of the reflected interfered light is given by [68, 69]

$$I = I_1 + I_2 + 2\sqrt{I_1 I_2}\cos\left(\frac{4\pi n\delta}{\lambda} + \varphi\right) \tag{6}$$

where I_1 and I_2 are the light intensities of the first and the second reflection, respectively; n is the refractive index of Fabry-Perot cavity medium, δ is the cavity length, λ is the optical wavelength, and φ is the initial phase difference.

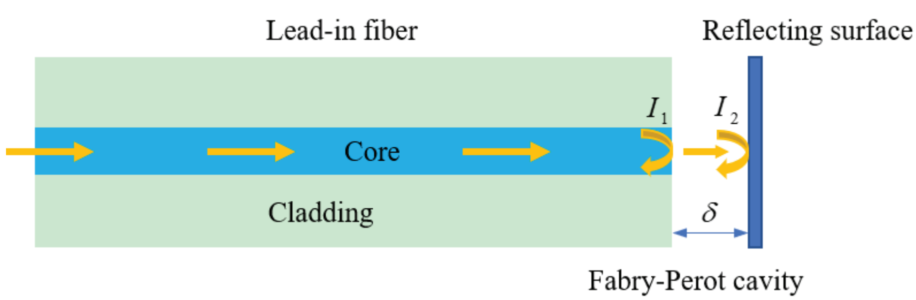

Fig. 8. Schematic illustration of the EFPI working principle.

As the Fabry-Perot cavity parameters (i.e. the cavity length or the refractive index of cavity medium) change due to external perturbation induced by strain, temperature, pressure, bending, concentration, or refractive indices, the interference signal intensity and the corresponding interference spectrum change accordingly. Therefore, these external parameters can be monitored by analyzing the change of Fabry-Perot cavity length based on intensity demodulation or phase demodulation technology.

5.2 EFPI fiber optic corrosion sensors

With a proper packaged structure, the EFPI sensor could be a good candidate for reinforcement steel corrosion monitoring in concrete structures. A specially designed EFPI sensor was embedded between two steel rebars to measure internal concrete cracking caused by corrosion expansion of these two rebars as shown in Fig. 9 [42]. The EFPI corrosion sensor is composed of two semi-reflective optical fibers separated by an air gap that can freely extend or retract. It was perpendicularly placed between the steel rebars where longitudinal cracks are likely to occur in a concrete beam [42]. With the development of steel corrosion, the EFPI sensor gradually elongates due to corrosion-induced concrete cracking. The relation between the EFPI strain data and the amount of corrosion-induced mass loss was experimentally established.

5.3 Performance of EFPI corrosion sensor

Only the EFPI fiber optic corrosion sensor proposed by Maalej et al. [24] was found in the literature. However, the sensor parameters such as sensitivity, monitoring range and service life were not discussed in the paper. As stated in previous section, monitoring of steel reinforcement corrosion by using the EFPI corrosion sensor as shown in Fig. 9 is realized by indirectly monitoring corrosion-induced internal concrete cracking. Therefore, the sensitivity is dependent on the relation between corrosion-induced mass loss of the reinforcement steel and the crack width, which varies from case to case due to non-homogeneity of concrete and randomness of steel corrosion. Therefore, the sensitivity of this EFPI corrosion sensor should be not high and its accuracy depends on factors such as steel bar corrosion morphology, reinforcement locations, and concrete properties. It is known that there are two stages of corrosion: corrosion initiation and corrosion propagation. Different from most FBG and LPFG corrosion sensors, which focus on the initiation and early corrosion propagation stage, this EFPI corrosion sensor only works after internal cracking of concrete. Therefore, the monitoring range should be the later corrosion propagation stage especially after concrete cracking. The service life is primarily dependent on the corrosion rate of the steel rebar after concrete cracking, as well as the growth rate of crack width in concrete.

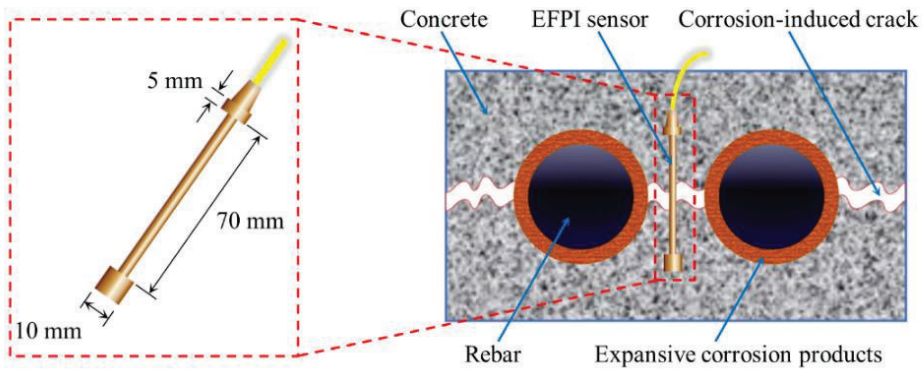

Fig. 9. Schematic illustration of EFPI corrosion sensor [24].

6. Brillouin backscattering-based distributed fiber corrosion sensors

Brillouin optical time domain reflectometry (BOTDR) and Brillouin optical time domain analysis (BOTDA) are two widely used distributed fiber sensing technologies based on Brillouin backscattering [70]. The following section focuses on distributed fiber optic corrosion sensors based on BOTDR and BOTDA.

6.1 Sensing principle of BOTDR and BOTDA

BOTDR-based fiber optic sensors operate based on spontaneous Brillouin scattering (SpBS), which is an inelastic scattering process due to the interaction of an incident light wave with thermally generated acoustic wave field in an optical fiber [71]. As illustrated in Fig. 10a, when an optical pulse is launched into the fiber and propagates forward, it will continuously produce spontaneous Brillouin backscattered light along the length. The distance between the position where the spontaneous Brillouin backscattered light is excited and the incident end of the fiber, denoted as u, can be expressed as:

$$u = \frac{ct}{2n} \tag{7}$$

where c is the light velocity in vacuum, t represents the time interval between the launching time of the optical pulse and the receiving time of the spontaneous Brillouin backscattered light at the incident end of the fiber, n is the fiber refractive index. Therefore, the spatial distribution of different locations of spontaneous Brillouin backscattered light excitement along the length of the fiber can be reconstructed by analyzing the time interval t corresponding to each specific location.

If the fiber is subjected to external interference such as strain or temperature change, a frequency shift will happen for the spontaneous Brillouin backscattered light, which is known as the Brillouin frequency shift ν_B. The Brillouin frequency shift due to changes of strain and temperature can be mathematically expressed as [71, 72]

$$\nu_B(T,\varepsilon) = C_T \Delta T + C_\varepsilon \Delta\varepsilon + \nu_0(T_0,\varepsilon_0) \tag{8}$$

where C_T and C_ε are the temperature and strain coefficient, respectively, ΔT is the temperature variation around the initial temperature T_0, $\Delta\varepsilon$ is the strain variation with respective to initial strain ε_0, $\nu_0(T_0,\varepsilon_0)$ is the reference frequency shift. Therefore, the strain and/or temperature distribution can be obtained by measuring the Brillouin frequency shift along the length of the fiber based on Eqs. (7) and (8).

BOTDA is a more complicated form of BOTDR, and it has a more intense detected signal since it uses stimulated Brillouin scattering through two counterpropagating light waves [73, 74]. Basic configuration of a typical BOTDA sensor is shown in Fig. 10b. In BOTDA technique [70, 75], two counterpropagating light waves including a pulse light (the pump) and a continuous wave light (the probe signal) are launched into the two ends of the sensing fiber, respectively. Stimulated Brillouin scattering occurs as the two light frequency differences equal the Brillouin frequency shift ν_B. Stimulated Brillouin scattering results in the maximum energy transfer from the pump to the probe signal, i.e., amplifying the probe signal. The distance z between the position where the probe signal is amplified and the fiber end where the pulse light is injected can be expressed as:

$$z = \frac{ct}{2n} \tag{9}$$

where c is the light velocity in vacuum, t represents the time interval between launching the pulse light and receiving the amplified probe signal at the fiber end where the pulse light is injected, n is the fiber refractive index. Therefore, the distribution of the locations where the probe signal is amplified along the fiber can be reconstructed by analyzing the time interval t based on Eq. (9).

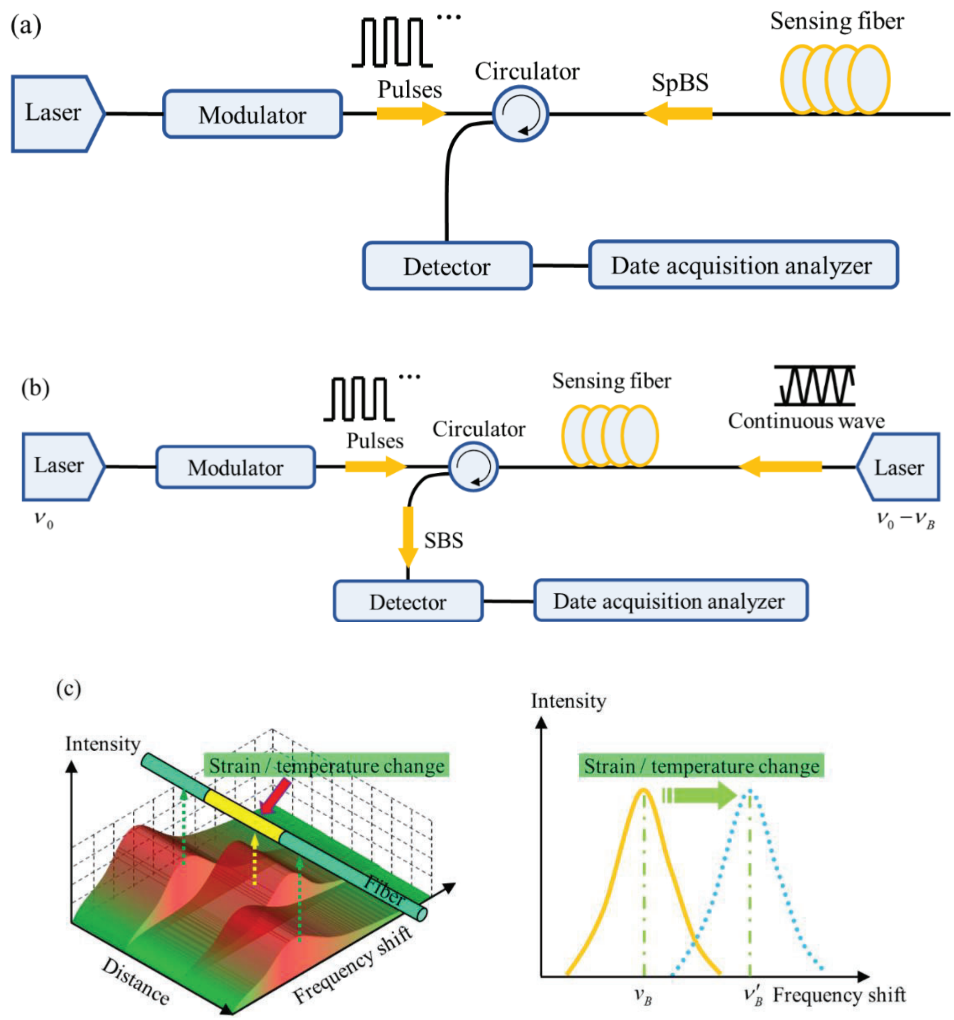

Fig. 10. Schematic illustration of sensing principle of Brillouin backscattering-based distributed fiber: Schematic diagram of the basic structure of the typical (a) BOTDR and (b)BOTDA sensor; (c) variations of the Brillouin frequency shift due to strain/ temperature changes

In addition, the amplification of the probe signal is also called Brillouin gain. Brillouin gain spectra is measured at a certain location by varying the frequency difference between the pump and the probe signal with an appropriate frequency interval [76]. The Brillouin frequency shift is directly obtained from Brillouin gain spectra according to the fact that the frequency difference corresponding to the maximum value of the Brillouin gain equals to the Brillouin frequency shift in Brillouin gain spectra. A schematic representation of the Brillouin frequency shift with varying with train/temperature change is illustrated in Fig. 10c. Therefore, the strain and/or temperature distribution can be obtained by measuring the Brillouin frequency shift at each location of the sensing optical fiber.

6.2 BOTDR/BOTDA fiber optic corrosion sensors

BOTDR offers the advantages of single-ended access and long-range sensing, while BOTDA requires two-sided access but has a more intense detected signal. Both sensor types have attracted research attention for corrosion monitoring of reinforcement steel in concrete over the past decade. Most of the BOTDR/BOTDA distributed fiber optic corrosion sensors are based on either measuring corrosion-induced volume expansion of steel bar or corrosion-induced concrete cracking. Sun et al. [33] employed BOTDR optical fiber to monitor corrosion initiation and concrete surface cracking by wrapping it around the surface of a small reinforced concrete column with polyurethane adhesive as shown in Fig. 11a. Results showed that this BOTDR fiber optic sensor could not only measure the strain but also be able to identify the crack locations. However, it is suitable for uniform corrosion monitoring, and the monitoring accuracy is affected by the thickness and properties of the concrete cover.

To protect the optical fiber from damage caused by chemical attack, mechanical impact, material deterioration and man-made interference, Mao et al. [77] proposed a method to seal BOTDA fiber optic sensors for monitoring large-scale civil structures. This sealing method embeds the BOTDA fiber in three steps: (1) embed small diameter tubes at desired location, (2) apply an air blowing technique to deploy the optical fiber inside the tubes, and (3) utilize a vacuum technique to tightly seal the optical fiber inside the tubes. The sealed BOTDA fiber optic sensor is schematically shown in Fig. 11b. It should be noted that this BOTDA seal method was designed for distributed strain measurement of large structures, and the corrosion test was intended to confirm its durability and stability in corrosive environments [94]. Mao et al. [54] also monitored reinforcement steel corrosion with combined BOTDA and FBG fiber optic sensors, and found that BOTDA could monitor concrete expansion and crack width, while FBG could identify the time and position of corrosion-induced concrete cracking. The thickness and properties of concrete cover affect the corrosion monitoring accuracy.

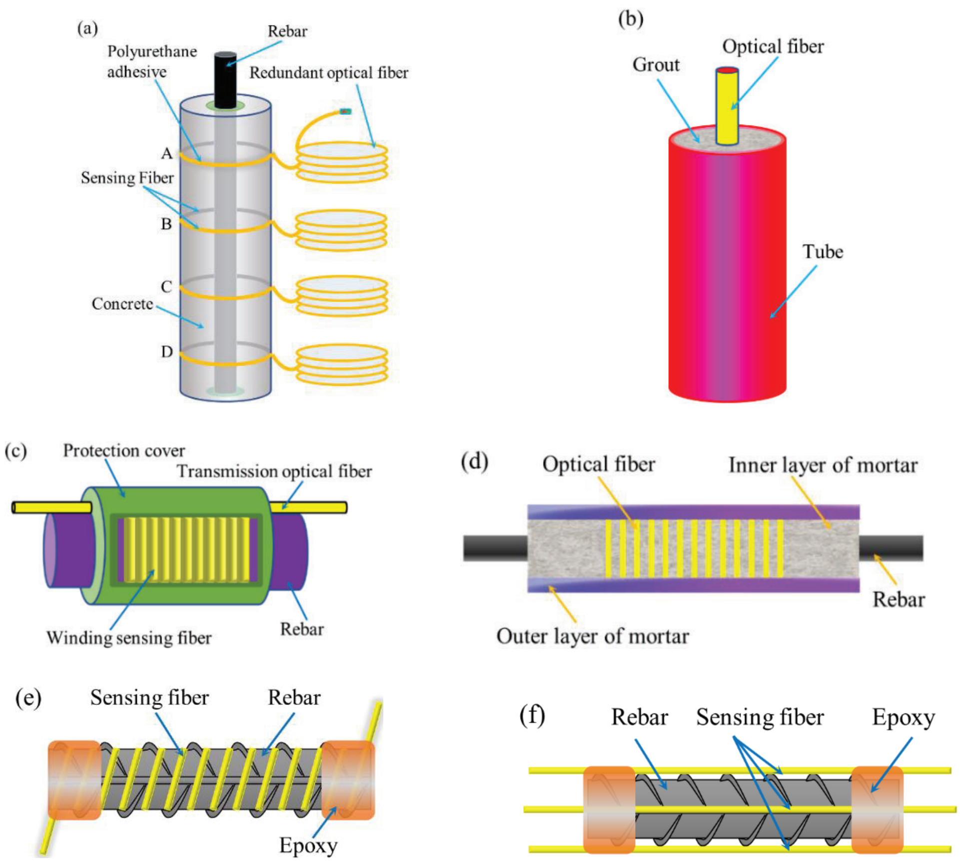

Fig. 11. Various types of Brillouin backscattering-based distributed fiber corrosion sensors: (a) optical fiber wrapped on the surface of a cylindrical concrete with a steel rebar in core [33], (b) optical fiber encased in a tube filled with grout [77], (c) coil-wound attached optical fiber on the surface of a steel rebar and covered with a porous soft material and chain link fence [28], (d) coil-wound attached optical fiber on the surface of a steel rebar and covered with two mortar layers [41], (e) PPP-BOTDA fiber wrapped around a steel rebar [43], and (f) PPP-BOTDA fiber attached on the surface of a steel rebar [43].

Zhao et al. [28] designed three types of BOTDA fiber optic corrosion sensors for reinforcement steel corrosion monitoring in reinforced concrete structures, one of which is shown in Fig. 11c. The optical fiber was coil-wound attached on the surface of a piece of steel rebar and then protected with a porous soft material and chain link fence. The corrosion of the steel rebar was monitored indirectly by measuring the strain in the fiber due to corrosion-induced volume expansion. Three years later in 2014, they found that this BOTDA fiber optic corrosion sensor can only be employed to monitor steel corrosion in early stage by comparing with a low-coherent fiber-optic strain sensor [78]. Therefore, in 2017, they proposed another BOTDA fiber optic corrosion sensor as shown in Fig. 11d [41]. Instead of protecting the fiber with porous soft material and chain link fence, two mortar layers were applied to cover the fiber wrapped around the steel bar surface. It is noted that the BOTDA fiber optic sensors proposed by Zhao et al. [28, 41, 78] only works for uniform corrosion monitoring as the measured strain is the averaged strain along the wrapped length. Moreover, the monitoring accuracy is also affected by the mechanical properties of the protective materials over the fiber.

Compared with traditional BOTDA, pulse pre-pump BOTDA (PPP-BOTDA) demonstrates a higher spatial resolution. Fan et al. [43, 79, 80] employed PPP-BOTDA optic fibers to monitor steel rebar corrosion by directly wrapping the fiber around the steel rebar (Fig. 11e) or attaching the fiber along the length of the steel rebar (Fig. 11f). With an increase of corrosion time, generation of corrosion products leads to a strain change in the fiber which was measured with a PPP-BOTDA data acquisition system. Compared with the parallel attachment along the length of the steel rebar, the spiral wrap method has a higher sensitivity and spatial resolution for corrosion monitoring. Moreover, the corrosion monitoring sensitivity of both cases is not affected by the concrete cover properties, but is influenced by the tightness of the fiber with the steel rebar.

6.3 Performance of BOTDR and BOTDA fiber optic corrosion sensors

Brillouin backscattering-based distributed fiber corrosion sensors monitor steel corrosion through indirectly measuring corrosion-induced volume expansion of steel rebar and concrete expansion or cracking. Therefore, the measurand of Brillouin based distributed fiber optic corrosion sensors is strain. In addition to the measurand, sensitivity, monitoring range, service life, and spatial resolution are also important parameters for distributed corrosion sensing. Table 4 summarizes the parameters of Brillouin based distributed fiber optic corrosion sensors proposed over the past two decades. The spatial resolution herein refers to the resolution of the fiber itself, which is dependent on the demodulation technique of the instrument. For corrosion monitoring of steel rebars, it also depends on the wrapping method of the fiber around the steel rebar. The spatial resolution of corrosion monitoring equals to the fiber resolution if the fiber is installed parallel to the direction of the steel rebar. However, if the fiber is spirally wrapped around the surface of a steel rebar or concrete cover, the spatial resolution of corrosion monitoring is also dependent on the wrapping spacing and the concrete cover thickness. The sensitivity is dependent on the transfer path of corrosion-induced volume expansion to the fiber core, and therefore is affected by the installation method and the mechanical properties of the materials between the steel rebar and the fiber core. The monitoring range is mainly dependent on the capacity of the demodulation instrument and the installation method. The service life is dependent on the corrosion rate of steel reinforcement, and it is also affected by the capacity of demodulation of optical instruments.

Table 4. Factors affecting the performance of Brillouin backscattering-based distributed fiber corrosion sensors.

Sensor	Measurand	Spatial resolution	Sensitivity	Experimentally observed monitoring range	Service life
Fig. 11a [33]	Strain	1.0 m	Depends on the thickness, porosity and properties of concrete cover, properties of polyurethane adhesive, wrap tightness of FBG fiber.	Depends on the demodulation technique, and is affected by concrete cover and polyurethane adhesive, 850 $\mu\varepsilon$ in [77].	Depends on the corrosion rate of steel rebar, demodulation technique, durability of polyurethane adhesive.
Fig. 11b [77]	Strain	0.5 m	Depends on the mechanical properties of tube and grout, as well as the interfacial bond of tube-grout-optical fiber.	Depends on the demodulation capacity of data acquisition system, up to 1800 $\mu\varepsilon$ in [77].	Depends on the corrosion rate of steel rebar, demodulation technique.
Fig. 11c [28]	Strain	1.0 m	Depends on the wrap tightness of fiber, and mechanical properties of protective cover.	Depends on the demodulation capacity of data acquisition system, up to 5690 $\mu\varepsilon$ in [28].	Depends on the corrosion rate of steel rebar, demodulation technique.
Fig. 11d [41]	Strain	0.5 m	Depends on the tightness of fiber wrap, thickness and mechanical properties of mortar cover.	Depends on the demodulation capacity of data acquisition system, up to 7100 $\mu\varepsilon$ in [41].	Depends on the corrosion rate of steel rebar, demodulation technique.
Fig. 11e [43]	Strain	2.0 cm	Depends on the spacing and tightness of wrap fiber, the interfacial properties between steel and concrete.	Depends on the demodulation capacity of data acquisition system, up to 6000 $\mu\varepsilon$ in [43].	Depends on the corrosion rate of steel rebar, demodulation capacity.
Fig. 11f [43]	Strain	2.0 cm	Depends on the spacing and tightness of fiber, the interfacial properties between steel rebar and concrete, as well as the distribution of corrosion.	Depends on the demodulation capacity of data acquisition system, up to 500 $\mu\varepsilon$ in [43].	Depends on the corrosion rate of steel rebar, demodulation technique.

7. Optical frequency domain reflectometry-based corrosion sensors

7.1 Sensing principle of OFDR

Optical frequency domain reflectometry (OFDR) operates based on Rayleigh backscattering, and the basic configuration of a typical OFDR fiber optic sensor is shown in Fig. 12. A continuous wave (CW) light from a swept-wavelength laser source with a time-linear sweep varying frequency is split into two light beams by a 3 dB coupler: one goes into the sensing fiber and the other goes into the reference fiber [22, 81]. The beam light propagating in the fiber will continuously produce Rayleigh backscattering along the length of the fiber due to presence of impurities and inhomogeneities. The Rayleigh backscattering light is mixed with the reference light beam at the coupler and is detected by a photon detector. The detected reflected light is a function of the beat frequency which is expressed as [81]

$$f_b = \gamma\tau = \gamma \frac{2nz}{c} \tag{10}$$

where n is the fiber refractive index, z is the distance from the incident end of the fiber, c is the light velocity in vacuum, γ represents the frequency sweep rate which is defined as $\gamma = \Delta f / t_s$, where Δf is the sweep span and t_s is the sweep time. It can be observed from equation (10) that the location of the backscattering light from any point along the fiber can be easily localized by the detected beat frequency.

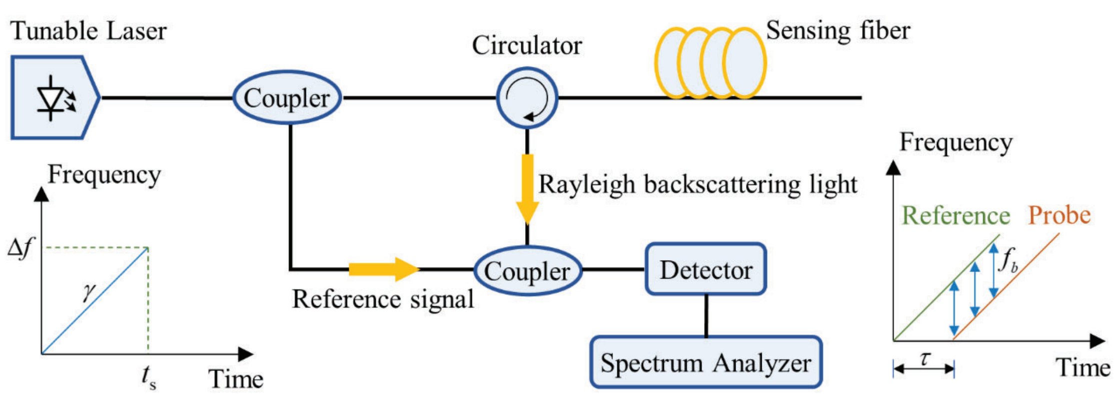

Fig. 12. Schematic illustration of the OFDR sensing principle.

The Rayleigh backscattering in the sensing fiber is affected by external parameter such as strain and temperature, both of which will cause a shift in the Rayleigh backscattered spectral and expressed as [82]

$$\frac{\Delta\lambda}{\lambda} = C_T \Delta T + C_\varepsilon \Delta\varepsilon \tag{11}$$

where λ is the signal wavelength, $\Delta\lambda$ is the backscattered spectral shift, C_T and C_ε are the temperature and strain coefficient, respectively, ΔT is the temperature variation, and $\Delta\varepsilon$ is the strain variation. Therefore, the strain and/or temperature distribution can be detected by measuring the Rayleigh backscattered spectral frequency shift at different locations along the sensing optical fiber.

7.2 OFDR fiber optic corrosion sensors

The OFDR fiber optic sensor is a good candidate for reinforcement steel corrosion monitoring because it possesses high monitoring range and spatial resolution compared with other fiber optic sensors. Corrosion monitoring with OFDR fiber optic sensors is based on measuring corrosion-induced volume expansion or concrete surface cracking. Magne et al. [42] cut a groove in a steel rebar and then periodically bonded an OFDR fiber with epoxy resin inside the groove for corrosion monitoring of the steel bar. As shown in Fig. 13a, this periodic arrangement of the OFDR fiber attachment in the steel rebar groove was intended to simultaneously monitor corrosion through unbonded sections and stress with bonded sections. Corrosion of steel rebar cause a volume expansion that exerts pressure against the unbonded fiber, which could be captured by an optical instrument.

Different from directly measuring corrosion-induced volume expansion of a steel rebar, corrosion-induced structural deterioration can be monitored indirectly through measuring stress or strain concentrations of the steel rebar after corrosion. Davis et al. [35, 83] installed nylon and polyimide coated fibers along the length of steel bars by using a cyanoacrylate adhesive to monitor effects of corrosion on the bond between concrete and steel as shown in Fig. 13b. This FOS system was also potentially able to locate sites of pitting corrosion that were visually hidden in the concrete by identifying the strain peaks. However, it is difficult to isolate the effects of pitting corrosion without prior knowledge of the pitting locations as pointed out by the authors [35]. Recently, Tang et al. [45, 84] employed OFDR fiber to monitor and localize initiation and propagation of corrosion-induced mortar surface cracking by directly wrapping and fixing the OFDR fiber around the surface of a reinforced mortar cylinder with epoxy resin as shown in Fig. 13c. The effects of fiber wrapping spacing on the sensitivity, monitoring range and service life were discussed.

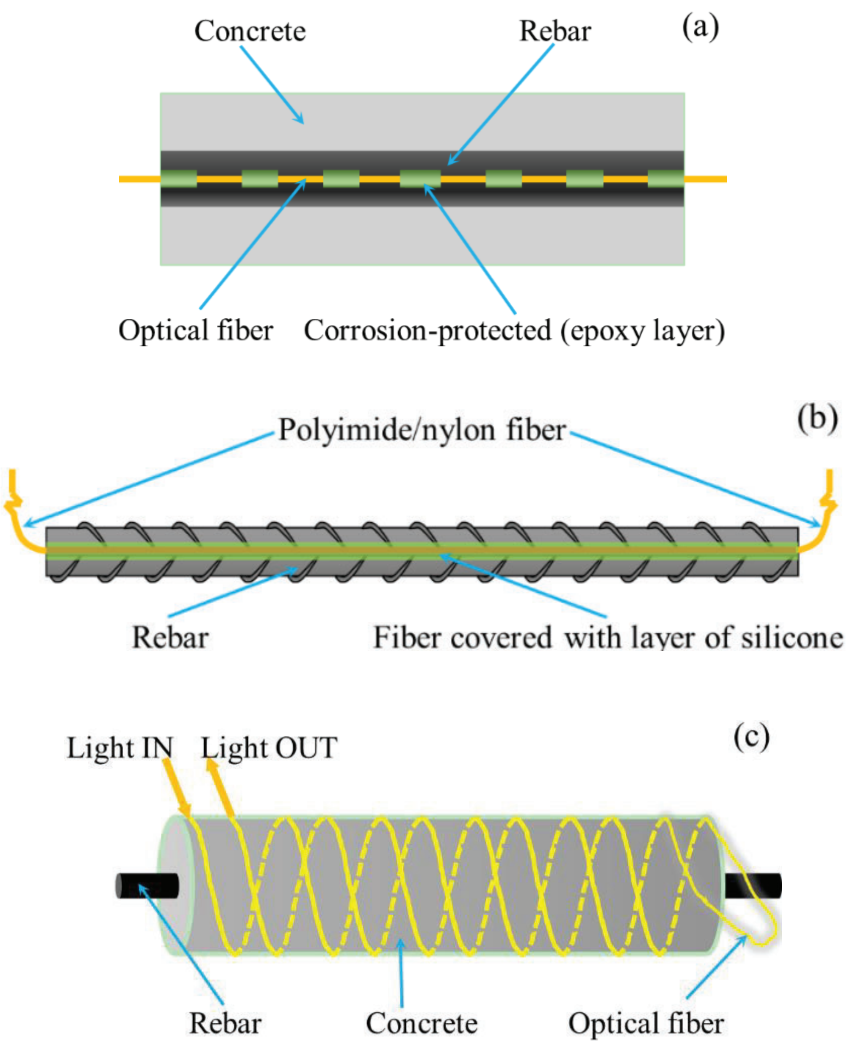

Fig. 13. OFDR based corrosion sensors: (a) periodical bonded OFDR fiber along the length of a steel bar [42], (b) complete bonded polyimide or nylon coated OFDR distributed fiber along the length of a steel bar [35], and (c) OFDR fiber wrapped on the concrete surface [45].

7.3 Performance of OFDR fiber optic corrosion sensors

The sensitivity of the OFDR corrosion sensor periodically bonded on the surface of a steel rebar proposed by Magne et al. [42] as shown in Fig. 13a is dependent on the tightness of unbonded fiber sections and the distance of the fiber from the rebar steel. Based on the configuration of the sensor design and corrosion monitoring principle, it can be inferred that the spatial resolution for corrosion monitoring is actually the length of the unbonded fiber segment. The monitoring range is dependent on demodulation capacity of the OFDR instrument and the properties of corrosion products that will exert pressure against the fiber. The service life is dependent on the corrosion rate of the steel rebar and the long-term performance of the epoxy adhesive. Regarding the OFDR distributed fiber optic corrosion sensors that are fully embedded or attached along the length of a steel rebar as investigated by Davis et al. and shown in Fig. 13b, the spatial resolution was reported to be 20 mm [35]. The corrosion monitoring sensitivity is primarily dependent on the strain transfer ratio from the rebar steel to the fiber through the epoxy layer, and is affected by the mechanical properties of epoxy resin and the interfacial bond strength of two interfaces: the interface between rebar steel and epoxy, and the interface between epoxy and optical fiber. The monitoring range is dependent on the maximum strain that the optical instrument can demodulate. The service life is dependent on the corrosion rate of the steel rebar and is affected by the long-term performance of epoxy adhesives.

The OFDR fiber optic corrosion sensor investigated by Tang et al. [45, 84] is actually a crack sensor, more specifically, a fiber optic sensor to monitor corrosion-induced concrete cracking. The sensitivity, spatial resolution, monitoring range and service life are discussed. The sensitivity is dependent on the fiber wrap spacing, the thickness and mechanical properties of the epoxy resin, the interfacial property between epoxy and mortar, as well as the properties of the fiber coating layer. The spatial resolution is the fiber wrap spacing and is limited by the diameter of the mortar specimens. The service life is dependent on the quality and durability of the epoxy resin, the capacity of the instrument, the diameter and corrosion rate of the steel bar, the fiber wrap spacing, as well as the thickness and properties of the mortar cover [45].

8. Other fiber optic corrosion sensors

8.1 Sensing principle

In addition to the aforementioned five types of fiber optic corrosion sensors, other optical fiber sensors have also been proposed for corrosion monitoring of reinforcement steel in concrete. Li et al. [85] proposed a fiber optic corrosion sensor by electroplating an Fe-C film on a metallized fiber core, and the output power of this fiber corrosion sensor increased by about 35% after the Fe-C film corroded as shown in Fig. 14a. Instead of correlating the corrosion loss with output power of an Fe-C coated fiber optic sensor, Cai et al. [86] established a relationship between the fractal dimension of corroded Fe-C film morphology and the output power of the fiber optic sensor. By coating an iron film on the end surface of an optical fiber, Leung and coworkers [87, 88] developed a fiber optic corrosion sensor for concrete structures and established a relation between the reflected signal of this sensor and the corrosion process of iron film as shown in Fig. 14b. Hu et al. [89, 90] proposed an Fe–C coated optical fiber polarizer for steel corrosion monitoring by depositing a thin layer of Fe–C film on side-polished fiber. By establishing a relation between the polarization characteristics and the corrosion condition of the Fe-C film, this fiber optic sensor could be used for corrosion monitoring in early stage as illustrated in Fig. 14c. Similar to iron or Fe-C coated cladding-etched FBG and LPFG fiber optics corrosion sensors, theses fiber optic corrosion sensors also have limited active service lives and are suitable for early stage corrosion monitoring of steel rebar.

Tang et al. [91] proposed an optical fiber assembly for long-term monitoring of pitting corrosion of steel rebars in concrete. The assembly consists of an array of optical fibers encased in steel straws (similar to Fig. 6f) with different wall thickness as shown in Fig. 14d. The steel straw has the same chemical composition as reinforcement steel in concrete. As corrosion pitting penetrates through the steel straw, the reflectivity of the encased optical fiber changes accordingly. Therefore, the assembly can be deployed in concrete for long-term corrosion monitoring by detecting the reflectivity change of each optical fiber. It is noted that this optical fiber corrosion assembly works for both uniform corrosion and pitting corrosion monitoring of steel rebar in concrete. In the case of pitting corrosion, it monitors the maximum pitting corrosion. The corrosion monitoring sensitivity is mainly dependent on the wall thickness difference of the steel straw, and the service life is primarily dependent on the maximum wall thickness.

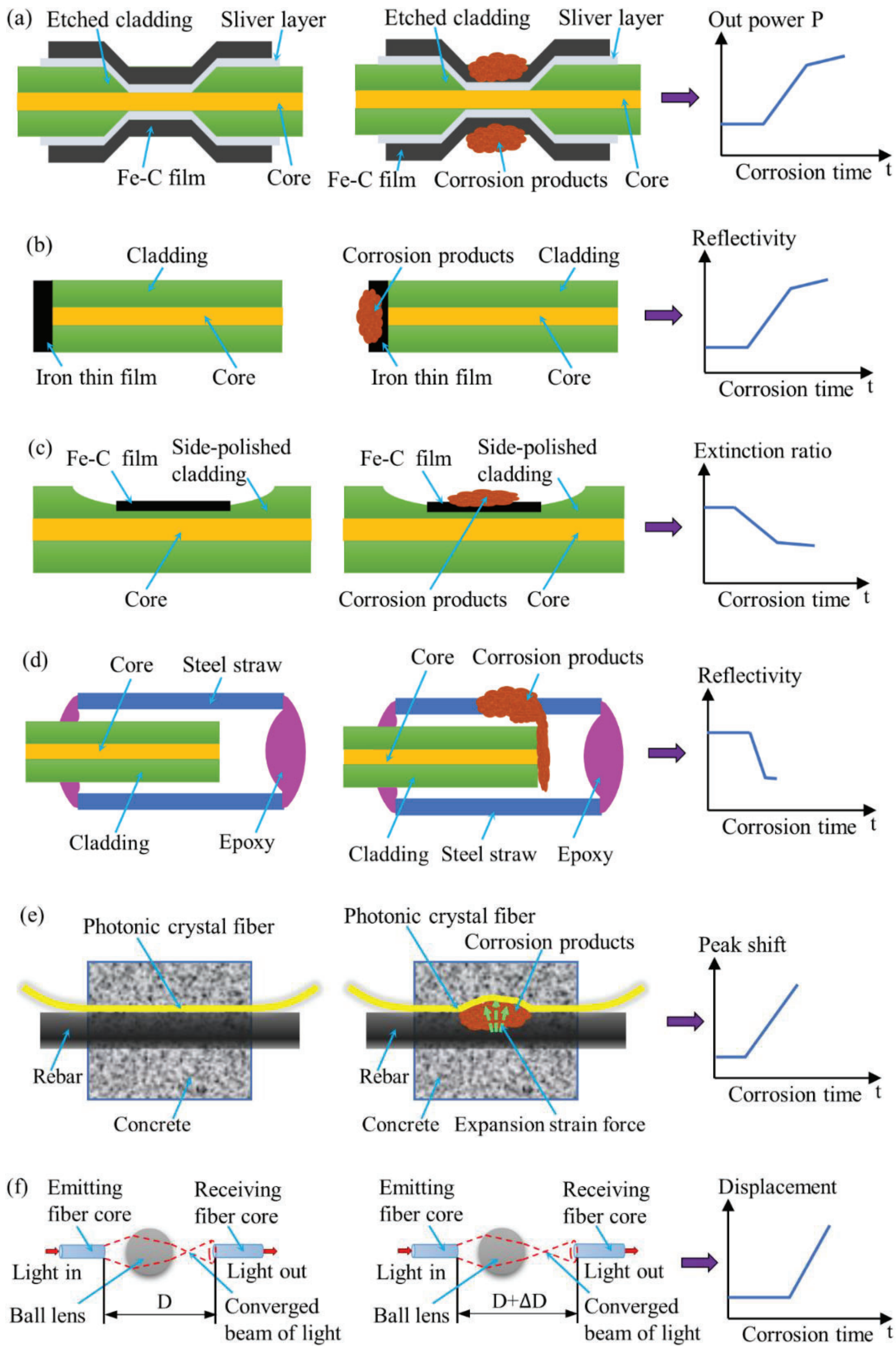

Fig. 14. Corrosion monitoring principle of other fiber optic corrosion sensors: (a) cladding-etched fiber coated with an inner layer of silver and an outside layer of Fe-C film [85], (b) fiber optic corrosion sensor with iron film coated end [87], (c) side-polished optical fiber coated with a Fe-C film [89], (d) optical fiber with one end embedded in a steel straw [91], (e) photonic crystal fiber corrosion sensor [92], and (f) lens-based plastic optical fiber corrosion sensor [93].

A fiber optic corrosion sensor was proposed for in-situ corrosion monitoring of reinforcement steel in concrete by using a fiber loop mirror system based on photonic crystal fibre (PCF) [92, 94]. This PCF fiber optic sensor is sensitive to external pressure and therefore, it is employed to monitor steel rebar corrosion by indirectly measuring the shift of peak wavelength of the transmission spectra due to corrosion-induced pressure as shown in Fig. 14e. The authors also mentioned that this sensor not only monitored corrosion but also could act as an ideal sensor for crack detection [92]. The sensitivity of the PCF fiber optic corrosion sensor for rebar corrosion monitoring in concrete is dependent on the relationship between the corrosion-induced mass loss of steel rebar and the expansive pressure of corrosion products against the surrounding concrete, which is affected by the mechanical properties of corrosion products and the surrounding concrete, as well as the porosity of interfacial transition zone (ITZ) between the steel rebar and the concrete.

Corrosion monitoring of steel rebars can also be realized by monitoring the chloride penetration in concrete. Wei et al. [95] proposed a fiber optic chloride sensor based on long period grating inscribed in a photonic crystal fiber coated with a layer of chloride sensitive film, and a relation between the chloride concentration and the shift of resonant wavelength was established. Fuhr et al. [96] proposed and investigated two optical fiber chloride sensors based on either fluorescence or absorption of the input light signal. The surface spectroscopy of steel reinforcement changes after corrosion, based on which a twin-fiber technique was proposed to monitor corrosion of steel rebars by Fuhr et al [97]. This technique employs two fibers: one fiber illuminates the surface of the steel rebar under investigation, and the other receives the reflected light (color modulated signal). A color shift in the input signal indicates corrosion. These fiber optic sensors are not applicable for corrosion monitoring of steel rebar due to carbonization of concrete cover. In the case of chloride-induced corrosion monitoring, they are suitable for monitoring corrosion initiation, but are not appropriate for corrosion monitoring in propagation stage since there is not obvious relationship between the chloride concentration and the corrosion rate or corrosion-induced mass loss of steel rebars.

Zhao et al. [98] proposed a fiber optic corrosion sensor based on white light interferometer technique for monitoring corrosion-induced expansion strain in concrete. The sensitivity of the proposed sensor was 3.3 με with a sensing length of 3 m, and the maximum strain measured due to steel corrosion was 1290 με. It is noted that this fiber optic corrosion sensor measures the average corrosion expansion strain, and its sensitivity is affected by the tightness of fiber wrap around the steel rebar, the properties of the protective materials over the fiber and the corrosion products. Recently, a lens-based plastic optical fiber (LPOF) sensor is proposed to monitor rebar corrosion as shown in Fig. 14f [93]. The LPOF fiber optic sensor has a ball lens located between the emitting fiber and the receiving fiber, the light emitted from the emitting fiber is converged to a focal point through the ball lens and then enters the receiving fiber. The light loss received by the received fiber increases with an increase of the distance between the receiving fiber and the ball lens, and therefore, it was deployed on the surface of concrete to monitor steel corrosion-induced concrete cover cracking.

8.2 Performance of other fiber optic corrosion sensors

For Fe-C or iron film coated optical fiber corrosion sensors as shown in Figs. 14a, 14b and 14c, the sensitivity, monitoring range and service life are all dependent on the thickness and porosity of Fe-C or iron film. Moreover, the service life is also affected by the corrosion rate of the Fe-C or iron film. For optical fibers encased in a steel straw as shown in Fig. 14d, the sensitivity, monitoring range and service life rely on the wall thickness of the steel straw, and the service life is also affected by the corrosion rate of the steel. Regarding the photonic crystal fiber (PCF) based corrosion sensor as shown in Fig. 14e, the sensitivity is dependent on the tightness of PCF fiber bonded on the surface of a steel rebar and the distance of corrosion sites from the PCF fiber. The monitoring range relies on the long-term performance of epoxy resin and the distance of corrosion sites from the PCF fiber, while the service life is dependent on both the corrosion rate of steel rebars and the long-term performance of epoxy resin. As for the LPOF corrosion sensor, the reported working range of this LPOF sensor is 20,000 με and is dependent on the gauge length. Similar to other fiber optic corrosion sensors mentioned in previous sections that monitor steel rebar corrosion by indirectly measuring corrosion-induced concreter cracking, the corrosion monitoring sensitivity of this LPOF sensor is also affected by the thickness and properties of the concrete cover, and it is suitable for later stage corrosion monitoring especially after concrete cracking. Another limitation of this LPOF corrosion sensor is that the accuracy of corrosion monitoring is affected by temperature [93]. The service life of this LPOF corrosion sensor is primarily dependent on the corrosion rate of steel rebars in concrete.

9. Utilization of monitoring data

Corrosion of reinforcement steel in concrete structures is a process that proceeds non-uniformly in space and over time, and therefore brings uncertainty for safety assessment of corrosion-induced deteriorating structural components or systems. Traditionally, safety assessment of structures subjected to corrosion attack is performed in a probabilistic manner by considering the corrosion effect as a random variable or random process [99-103]. However, these probabilistic models are mostly established based on data from either accelerated corrosion test in the laboratory or field test of other structures, which do not reflect the actual condition of the structures under evaluation.

Based on review and discussion of various fiber optic corrosion sensors mentioned in previous sections, two types of corrosion-induced parameter changes are generally monitored by these sensors: optical properties of the surrounding environment (e.g., refractive index) and physical properties of steel reinforcement or surrounding concrete (e.g., volume expansion of steel rebars, concrete expansion/cracking). For these corrosion sensors based on the change in the refractive index of the surrounding environment such as cladding-etched FBGs and Fe-C coated LPFGs, they are sensitive to the surrounding environment and are suitable for corrosion monitoring at early stages or the penetration process of corrosive chemicals in the corrosion initiation stage. The corrosion information collected by these sensors could include chloride concentration, passive film thickness, time of corrosion onset, and so on. For optic fiber corrosion sensors based on volume expansion of steel rebars or concrete such as FBG corrosion sensors wrapped on the surface of steel rebars, EFPI corrosion sensor, BOTDR/BOTDA/OFDR distributed optic fiber corrosion sensors, they are suitable for corrosion propagation stage monitoring. The corrosion information collected includes volume of corrosion products, cross-sectional area loss of steel rebar, steel-concrete interfacial degradation, concrete cracking (number of cracks, crack width and length), and so on.

As fiber optic corrosion sensors are installed in structures under monitoring, the corrosion information collected from these sensors reflects the real-time corrosion status of the structure, and therefore can be used for model updating which significantly increases the accuracy of safety assessment. For example, the time of corrosion onset which is considered to be the termination of service life of the Hong Kong-Zhuhai-Macau bridge from the perspective of durability design could be accurately predicted with Fe-C coated LPFG sensors, and the serviceability of reinforced concrete structures subjected to corrosion attack could be determined by using OFDR distributed fiber optic sensors deployed on the surface of the concrete cover.

10. Future perspectives and challenges

Although many efforts have been made for the development of fiber optic sensors for reinforcement steel corrosion monitoring over the past two decades, there are still some aspects that need further exploration and improvement.

First, packaging techniques or methods are required that allow practical engineering applications. Most of the fiber optic corrosion sensors need to be installed on the surface of steel reinforcement cages and, therefore, robust packing techniques are necessary to prevent damage during concrete pouring and subsequent vibration.

Second, temperature and stress compensation techniques are to be developed further. To some extent, these sensors are affected by temperature variation. Therefore, temperature compensation is needed for those that are sensitive to temperature change such as FBG-based fiber optic corrosion sensors. Besides, the steel reinforcement is subjected to tensile or compression stresses in reinforced concrete structures, hence the strain generated due to structural loading also influences these sensors [104].

Third, determination of sensor parameters such as sensitivity, monitoring range and service life are required to allow for optimal design of monitoring systems. Sensitivity is one of the most important parameters for sensors and sensing instruments. However, the sensitivity of most of the fiber optic corrosion sensors reviewed in this work is not well defined. Monitoring range and service life are also two important parameters that are often not well specified. Monitoring range should be defined in terms of corrosion mass, loss and this is difficult for those sensors that monitor corrosion indirectly. Service life not only depends on the sensor itself but also on the corrosion rate of the steel rebar on site.

Last but not least, systems for efficient networking of fiber optic corrosion sensors are to developed. Civil engineering structures such as bridges and tunnels are usually large-scale structures and corrosion of steel is not uniformly distributed in space and over time. Therefore, networking of fiber optic corrosion sensors needs to be developed for acquisition of corrosion data over the relevant parts of the entire structure and used for accurate assessment of structural performance. Acquisition of corrosion data needs optical sensing instruments, and different sensors need different instruments, which are usually expensive. Therefore, an optical instrument that has multi-channels and is compatible with all fiber optic corrosion sensors is also an indispensable part of the sensor networking.

11. Conclusions

In this work, a state-of-the-art review on fiber optic sensors for corrosion monitoring of reinforcement steel in concrete structures is presented. The fiber optic corrosion sensors reviewed include FBG corrosion sensors, LPFG corrosion sensors, EFPI corrosion sensors, Brillouin backscattering-based distributed fiber optic corrosion sensors, OFDR distributed corrosion sensors, and other fiber optic corrosion sensors. The corrosion sensing principles are introduced, and the performance parameters including sensitivity, monitoring range and service life are discussed. The utilization of monitoring data, future perspective and challenges are discussed. Based on review and discussion, the following conclusions can be drawn:

(1) For FBG fiber optic sensors either coated or uncoated based on monitoring corrosion-associated chemical reactions near the rebar or inside the coating layer, the sensitivity and monitoring range is mainly dependent on the distance of the fiber from the corroding sites or the thickness and properties of the coating layer, and the service life is primarily dependent on the corrosion rate of the coating layers (Fe-C coating,

iron film) and the steel rebar. They are suitable for early stage corrosion monitoring of reinforcement steel in concrete structures.

(2) A second category of FBG fiber optic corrosion sensors are based on monitoring strains due to volume expansion of the steel rebar or concrete expansion/cracking. The sensitivity and monitoring range is dependent on the strain transfer coefficient between volume expansion and fiber strain, which is affected by the wrap tightness of the FBG fiber around the surface of the steel rebar or concrete cover, the properties of surrounding concrete, corrosion products, packaging method, and properties of packaging materials. The service life is primarily dependent on the corrosion rate of the steel rebar, and is affected by the demodulation capacity of the optical instrument. They are suitable for later stage corrosion monitoring of reinforcement steel in concrete structures.

(3) The measurand of all proposed LPFG fiber optic corrosion sensors is the refractive index. For LPFG fiber sensors merged in phenolic resin or encased in a steel straw, the sensitivity is dependent on the thickness and properties of phenolic resin or straw steel, and the service life is primarily dependent on the corrosion rate of steel rebar or steel straw. For LPFG fiber sensors coated with nanoparticle filled polyurethane or Fe-C coatings, both the sensitivity and monitoring range are dependent on the thickness and properties of coating layers. The service life is dependent on the corrosion rate and total mass of nano iron particle or Fe-C coatings. The LPFG fiber optic corrosion sensors coated with a thin Fe-C layer are suitable for passivation or early stage corrosion monitoring of steel rebars in concrete.

(4) The EFPI fiber optic corrosion sensor is actually a crack sensor that monitors corrosion-induced concrete cracking. The sensitivity and monitoring range is significantly affected by the location of the sensor with respect to the steel rebars and the properties of the surrounding concrete, and the service life is dependent on the corrosion rate of the steel rebars. It is suitable for corrosion monitoring in the propagation stage especially after concrete cracking.

(5) BOTDR/BOTDA/OFDR distributed fiber optic corrosion sensors monitor reinforcement steel corrosion by indirectly measuring strains from volume expansion of steel rebars or corrosion-induced

concrete expansion/cracking. The sensitivity and monitoring range are dependent on the transfer coefficient between the volume expansion of corrosion products and the fibers, which is affected by the installation methods, properties of installation materials, and demodulation capacity of optical instruments. The service life is dependent on the corrosion rate of the steel rebar and the demodulation capacity.

(6) The data collected from the fiber optic corrosion sensors include passive film thickness, corrosion initiation time, chloride penetration, mass loss of steel rebar, cracking width of concrete, and so on. Hence, most of them are tailored towards being effective in a specific stage of the corrosion process, and efficient networking of fiber optic corrosion sensors is to be developed. The monitoring data from these sensor networks can be used to increase the accuracy of safety assessment or prediction of service life.

Declaration of Competing Interest

The authors declare that they have no known competing financial interests or personal relationships that could have appeared to influence the work reported in this paper.

Acknowledgements

This work was supported by the National Natural Science Foundation of China (No. 51878119, 52111540162, 51421064), and Natural Science Foundation of Liaoning Province (No. 2020-MS-121).

References

[1] B.R. Sweeney, Designing Port Infrastructure for Sea Level Change: A Survey of US Engineers, 15th Triennial International Conference on Ports - Connect Innovate Transform, Amer Soc Civil Engineers, Pittsburgh, PA, 2019, pp. 477-488.

[2] Q. Li, K. Li, X. Zhou, Q. Zhang, Z. Fan, Model-based durability design of concrete structures in Hong Kong–Zhuhai–Macau sea link project, Structural Safety 53 (2015) 1-12.

[3] B. Hou, X. Li, X. Ma, C. Du, D. Zhang, M. Zheng, W. Xu, D. Lu, F. Ma, The cost of corrosion in China, NPJ Mater. Degrad. 1(1) (2017) 10.

[4] Highways and Bridges, 2021. https://www.nace.org/resources/industries-nace-serves/highways-bridges. (Accessed 17 June 2021).

[5] D. Malomo, N. Scattarreggia, A. Orgnoni, R. Pinho, M. Moratti, G.M. Calvi, Numerical study on the collapse of the morandi bridge, J. Perform. Constr. Facil. 34(4) (2020) 13.

[6] 2021. https://www.abc.net.au/news/2021-07-27/miami-building-collapse-last-remains-death-toll-98/100326330. (Accessed October 15 2021).

[7] M.F. Montemor, A.M.P. Simoes, M.G.S. Ferreira, Chloride-induced corrosion on reinforcing steel: from the fundamentals to the monitoring techniques, Cement and Concrete Composites 25(4-5) (2003) 491-502.

[8] C. Andrade, C. Alonso, Corrosion rate monitoring in the laboratory and on-site, Constr. Build. Mater. 10(5) (1996)

315-328.
[9] S. Kessler, C. Gehlen, Reliability Evaluation of Half-Cell Potential Measurement Using POD, J. Infrastruct. Syst. 23(2) (2017) 6.
[10] A.A. Sagues, M.T. Walsh, Kelvin Probe electrode for contactless potential measurement on concrete - Properties and corrosion profiling application, Corrosion Sci. 56 (2012) 26-35.
[11] Z. Li, Z. Jin, P. Wang, T. Zhao, Corrosion mechanism of reinforced bars inside concrete and relevant monitoring or detection apparatus: A review, Constr. Build. Mater. 279 (2021) 14.
[12] H. Nasser, C. Van Steen, L. Vandewalle, E. Verstrynge, An experimental assessment of corrosion damage and bending capacity reduction of singly reinforced concrete beams subjected to accelerated corrosion, Constr. Build. Mater. 286 (2021) 122773.
[13] C. Van Steen, H. Nasser, E. Verstrynge, M. Wevers, Acoustic emission source characterisation of chloride-induced corrosion damage in reinforced concrete, Struct. Health Monit. 21.
[14] C. Van Steen, L. Pahlavan, M. Wevers, E. Verstrynge, Localisation and characterisation of corrosion damage in reinforced concrete by means of acoustic emission and X-ray computed tomography, Constr. Build. Mater. 197 (2019) 21-29.
[15] A. Zaki, H.K. Chai, D.G. Aggelis, N. Alver, Non-Destructive Evaluation for Corrosion Monitoring in Concrete: A Review and Capability of Acoustic Emission Technique, Sensors 15(8) (2015) 19069-19101.
[16] H. Li, D. Li, G. Song, Recent applications of fiber optic sensors to health monitoring in civil engineering, Eng. Struct. 26(11) (2004) 1647-1657.
[17] B. Lee, Review of the present status of optical fiber sensors, Opt. Fiber Technol. 9(2) (2003) 57-79.
[18] L. Fan, Y. Bao, Review of fiber optic sensors for corrosion monitoring in reinforced concrete, Cement and Concrete Composites 120 (2021) 104029.
[19] B. Culshaw, A. Kersey, Fiber-optic sensing: A historical perspective, Journal of Lightwave Technology 26(9) (2008) 1064-1078.
[20] J.K. Sahota, N. Gupta, D. Dhawan, Fiber Bragg grating sensors for monitoring of physical parameters: a comprehensive review, Opt. Eng. 59(6) (2020) 35.
[21] S.W. James, R.P. Tatam, Optical fibre long-period grating sensors: Characteristics and application, Meas. Sci. Technol. 14(5) (2003) R49-R61.
[22] P. Lu, N. Lalam, M. Badar, B. Liu, B.T. Chorpening, M.P. Buric, P.R. Ohodnicki, Distributed optical fiber sensing: Review and perspective, Appl. Phys. Rev. 6(4) (2019) 35.
[23] K.D. Bennett, L.R. McLaughlin, Monitoring of corrosion in steel structures using optical fiber sensors, Spie-Int Soc Optical Engineering, Bellingham, 1995.
[24] M. Maalej, S.F.U. Ahmed, K.S.C. Kuang, P. Paramasivam, Fiber optic sensing for monitoring corrosion-induced damage, Struct. Health Monit. 3(2) (2004) 165-176.
[25] Z. Zheng, X. Sun, Y. Lei, Monitoring corrosion of reinforcement in concrete structures via fiber Bragg grating sensors, Frontiers of Mechanical Engineering in China 4(3) (2009) 316-19.
[26] S.K.T. Grattan, S.E. Taylor, T. Sun, P.A.M. Basheer, K.T.V. Grattan, Monitoring of corrosion in structural reinforcing bars: performance comparison using in situ fiber-optic and electric wire strain gauge systems, IEEE Sens. J. 9(11) (2009) 1494-1502.
[27] J. Gao, J. Wu, J. Li, X. Zhao, Monitoring of corrosion in reinforced concrete structure using Bragg grating sensing, NDT E Int. 44(2) (2011) 202-205.
[28] X. Zhao, P. Gong, G. Qiao, J. Lu, X. Lv, J. Ou, Brillouin corrosion expansion sensors for steel reinforced concrete structures using a fiber optic coil winding method, Sensors 11(11) (2011) 10798-10819.
[29] W. Hu, H. Cai, M. Yang, X. Tong, C. Zhou, W. Chen, Fe-C-coated fibre Bragg grating sensor for steel corrosion monitoring, Corrosion Sci. 53(5) (2011) 1933-1938.
[30] H. Liu, D. Liang, J. Zeng, J. Jin, J. Wu, J. Geng, Design of a long-period fiber grating sensor for reinforcing bar corrosion in concrete, J. Intell. Mater. Syst. Struct. 23(1) (2012) 45-51.
[31] M.R. Abu Hassan, M.H. Abu Bakar, K. Dambul, F.R.M. Adikan, Optical-based sensors for monitoring corrosion of reinforcement rebar via an etched cladding Bragg grating, Sensors 12(11) (2012) 15820-15826.
[32] Y. Huang, Z. Gao, G. Chen, H. Xiao, Long period fiber grating sensors coated with nano iron/silica particles for corrosion monitoring, Smart Mater. Struct. 22(7) (2013) 8.
[33] Y. Sun, B. Shi, S. Chen, H. Zhu, D. Zhang, Y. Lu, Feasibility study on corrosion monitoring of a concrete column with central rebar using BOTDR, Smart. Struct. Syst. 13(1) (2014) 41-53.
[34] N. Zhang, W. Chen, X. Zheng, W. Hu, M. Gao, Optical sensor for steel corrosion monitoring based on etched fiber Bragg grating sputtered with iron film, IEEE Sens. J. 15(6) (2015) 3551-3556.
[35] M. Davis, N.A. Hoult, A. Scott, Distributed strain sensing to determine the impact of corrosion on bond

performance in reinforced concrete, Constr. Build. Mater. 114 (2016) 481-491.
[36] W. Li, S.C.M. Ho, G. Song, Corrosion detection of steel reinforced concrete using combined carbon fiber and fiber Bragg grating active thermal probe, Smart Mater. Struct. 25(4) (2016) 9.
[37] C.H. Tan, Y.G. Shee, B.K. Yap, F.R.M. Adikan, Fiber Bragg grating based sensing system: Early corrosion detection for structural health monitoring, Sens. Actuator A-Phys. 246 (2016) 123-128.
[38] Y. Chen, F. Tang, Y. Bao, Y. Tang, G. Chen, A Fe-C coated long-period fiber grating sensor for corrosion-induced mass loss measurement, Opt. Lett. 41(10) (2016) 2306-2309.
[39] O. Almubaied, H.K. Chai, M.R. Islam, K.S. Lim, C.G. Tan, Monitoring corrosion process of reinforced concrete structure using FBG strain sensor, IEEE Trans. Instrum. Meas. 66(8) (2017) 2148-2155.
[40] F. Tang, Y. Chen, Y. Tang, Z.C. Li, G. Chen, Steel corrosion monitoring in concrete slab using a long period fiber grating assembly, CORROSION 2017, New Orleans, LA, USA, 2017.
[41] H. Lv, X. Zhao, Y. Zhan, P. Gong, Damage evaluation of concrete based on Brillouin corrosion expansion sensor, Constr. Build. Mater. 143 (2017) 387-394.
[42] S. Magne, S.A. Alvarez , S. Rougeault, Distributed Corrosion Detection using Dedicated Optical Fiber Sensor (OFS) based Steel Rebar within Reinforced Concrete Structures by Optical Frequency-Domain Reflectometry (OFDR), 9th European Workshop on Structural Health Monitoring, Manchester, United Kingdom, 2018.
[43] L. Fan, Y. Bao, G. Chen, Feasibility of distributed fiber optic sensor for corrosion monitoring of steel bars in reinforced concrete, Sensors 18(11) (2018) 15.
[44] C. Guo, L. Fan, C. Wu, G. Chen, W. Li, Ultrasensitive LPFG corrosion sensor with Fe-C coating electroplated on a Gr/AgNW film, Sens. Actuator B-Chem. 283 (2019) 334-342.
[45] F. Tang, L. Zhao, H. Tian, H. Li, H. Li, Localization and monitoring of initiation and propagation of corrosion-induced mortar cracking based on OFDR distributed optical fiber sensor, J. Intell. Mater. Syst. Struct. (2021) 1045389X20986996.
[46] R. Kashyap, Fiber bragg gratings, Academic press 2009.
[47] A.D. Kersey, M.A. Davis, H.J. Patrick, M. LeBlanc, K.P. Koo, C.G. Askins, M.A. Putnam, E.J. Friebele, Fiber grating sensors, Journal of Lightwave Technology 15(8) (1997) 1442-1463.
[48] A. Othonos, K. Kalli, D. Pureur, A. Mugnier, Fibre bragg gratings, Wavelength Filters in Fibre Optics, Springer, Berlin, 2006, pp. 189-269.
[49] C.H. Tan, F.R.M. Adikan, Y.G. Shee, B.K. Yap, Non-destructive fiber Bragg grating based sensing system: Early corrosion detection for structural health monitoring, Sens. Actuator A-Phys. 268 (2017) 61-67.
[50] Z. Zheng, Y. Lei, X. Sun, Measuring corrosion of steel in concrete via fiber bragg grating sensors-lab experimental test and in-field application, Earth And Space 2010: Engineering, Science, Construction, And Operations In Challenging Environments, 2010, pp. 2422-2430.
[51] W. Chen, X. Dong, Modification of the wavelength-strain coefficient of FBG for the prediction of steel bar corrosion embedded in concrete, Opt. Fiber Technol. 18(1) (2012) 47-50.
[52] S.K.T. Grattan, S.E. Taylor, T. Sun, P.A.M. Basheer, K.T.V. Grattan, In situ cross-calibration of in-fiber Bragg grating and electrical resistance strain gauges for structural monitoring using an extensometer, IEEE Sens. J. 9(11) (2009) 1355-1360.
[53] L. Sun, C. Li, C. Zhang, Z. Su, C. Chen, Early monitoring of rebar corrosion evolution based on FBG sensor, Int. J. Struct. Stab. Dyn. 18(8) (2018) 11.
[54] J. Mao, J. Chen, L. Cui, W. Jin, C. Xu, Y. He, Monitoring the corrosion process of reinforced Concrete using BOTDA and FBG sensors, Sensors 15(4) (2015) 8866-8883.
[55] W. Li, C. Xu, S.C.M. Ho, B. Wang, G. Song, Monitoring concrete deterioration due to reinforcement corrosion by integrating acoustic emission and FBG strain measurements, Sensors 17(3) (2017) 12.
[56] A.M. Vengsarkar, P.J. Lemaire, J.B. Judkins, V. Bhatia, T. Erdogan, J.E. Sipe, Long-period fiber gratings as band-rejection filters, Journal of Lightwave Technology 14(1) (1996) 58-65.
[57] V. Bhatia, Applications of long-period gratings to single and multi-parameter sensing, Opt. Express 4(11) (1999) 457-466.
[58] Y. Huang, F.J. Tang, X. Liang, G.D. Chen, H. Xiao, F. Azarmi, Steel bar corrosion monitoring with long-period fiber grating sensors coated with nano iron/silica particles and polyurethane, Struct. Health Monit. 14(2) (2015) 178-189.
[59] F. Tang, Y. Chen, Z. Li, Y. Tang, G. Chen, Application of Fe-C coated LPFG sensor for early stage corrosion monitoring of steel bar in RC structures, Constr. Build. Mater. 175 (2018) 14-25.
[60] Y. Chen, F. Tang, Y. Bao, G. Chen, Corrosion monitoring of steel bars embedded in mortar using Fe-C coated long period fiber gratings, CORROSION 2015, Dallas, Texas, USA, 2015.
[61] Y. Chen, F. Tang, Y. Tang, M.J. O'Keefe, G. Chen, Mechanism and sensitivity of Fe-C coated long period fiber

grating sensors for steel corrosion monitoring of RC structures, Corrosion Sci. 127 (2017) 70-81.
[62] F. Tang, Z. Li, C. Li, Y. Chen, H. Li, Monitoring passivation, pitting corrosion initiation, and propagation of steel bar with iron-carbon electroplated long period fiber-grating sensor, J. Mater. Civ. Eng. 32(12) (2020) 13.
[63] F. Tang, Z. Li, Y. Chen, H. Li, J. Huang, M.J. O'Keefe, Monitoring passive film growth on steel using Fe-Ccoated long period grating fiber sensor, IEEE Sens. J. 19(16) (2019) 6748-6755.
[64] C. Guo, L. Fan, G. Chen, Corrosion-induced mass loss measurement under strain conditions through gr/agnw-based, Fe-C coated LPFG sensors, Sensors 20(6) (2020) 17.
[65] Z. Fang, K.K. Chin, R. Qu, H. Cai, Fundamentals of optical fiber sensors, John Wiley & Sons 2012.
[66] A.L. Kalamkarov, S.B. Fitzgerald, D.O. MacDonald, The use of Fabry Perot fiber optic sensors to monitor residual strains during pultrusion of FRP composites, Compos. Pt. B-Eng. 30(2) (1999) 167-175.
[67] V. Bhatia, K.A. Murphy, R.O. Claus, M.E. Jones, J.L. Grace, T.A. Tran, J.A. Greene, Optical fibre based absolute extrinsic Fabry-Perot interferometric sensing system, Meas. Sci. Technol. 7(1) (1996) 58-61.
[68] Y. Du, Y. Chen, Y. Zhuang, C. Zhu, F. Tang, J. Huang, Probing nanostrain via a mechanically designed optical fiber interferometer, IEEE Photonics Technol. Lett. 29(16) (2017) 1348-1351.
[69] F. Tang, Z.C. Li, Y. Tang, Y. Chen, H. Li, Simultaneous measurement of shrinkage and coefficient of thermal expansion of mortar based on EFPI sensors with nanometer resolution, Measurement 152 (2020) 10.
[70] C. Hong, Y. Zhang, G. Li, M. Zhang, Z. Liu, Recent progress of using Brillouin distributed fiber optic sensors for geotechnical health monitoring, Sens. Actuator A-Phys. 258 (2017) 131-145.
[71] Q. Bai, Q. Wang, D. Wang, Y. Wang, Y. Gao, H. Zhang, M. Zhang, B. Jin, Recent advances in brillouin optical time domain reflectometry, Sensors 19(8) (2019) 45.
[72] T. Horiguchi, K. Shimizu, T. Kurashima, M. Tateda, Y. Koyamada, Development of a distributed sensing technique using brillouin-scattering, Journal of Lightwave Technology 13(7) (1995) 1296-1302.
[73] A. Masoudi, T.P. Newson, Contributed review: distributed optical fibre dynamic strain sensing, Rev. Sci. Instrum. 87(1) (2016) 9.
[74] K.K.K. Annamdas, V.G.M. Annamdas, Review on developments in fiber optical sensors and applications, in: A. Mendez, H.H. Du, A. Wang, E. Udd, S.J. Mihailov (Eds.), Fiber Optic Sensors and Applications Vii, Spie-Int Soc Optical Engineering, Bellingham, 2010.
[75] T. Horiguchi, M. Tateda, BOTDA-nondestructive measurement of single-mode optical fiber attenuation characteristics using brillouin interaction-theory, Journal of Lightwave Technology 7(8) (1989) 1170-1176.
[76] T. Kurashima, T. Horiguchi, M. Tateda, Distributed-temperature sensing using stimulated brillouin-scattering in optical silica fibers, Opt. Lett. 15(18) (1990) 1038-1040.
[77] J. Mao, W. Jin, Y. He, D. Cleland, Y. Bai, A novel method of embedding distributed optical fiber sensors for structural health monitoring, Smart Mater. Struct. 20(12) (2011) 9.
[78] H. Wei, X. Zhao, X. Kong, P. Zhang, Y. Cui, C. Sun, The performance analysis of distributed brillouin corrosion sensors for steel reinforced concrete structures, Sensors 14(1) (2014) 431-442.
[79] L. Fan, Y. Bao, W. Meng, G. Chen, In-situ monitoring of corrosion-induced expansion and mass loss of steel bar in steel fiber reinforced concrete using a distributed fiber optic sensor, Compos. Pt. B-Eng. 165 (2019) 679-689.
[80] L. Fan, X. Tan, Q. Zhang, W. Meng, G. Chen, Y. Bao, Monitoring corrosion of steel bars in reinforced concrete based on helix strains measured from a distributed fiber optic sensor, Eng. Struct. 204 (2020) 10.
[81] W. Eickhoff, R. Ulrich, Optical frequency-domain reflectometry in single-mode fiber, Appl. Phys. Lett. 39(9) (1981) 693-695.
[82] L. Wong, W.K. Chiu, J. Kodikara, Using distributed optical fibre sensor to enhance structural health monitoring of a pipeline subjected to hydraulic transient excitation, Struct. Health Monit. 17(2) (2018) 298-312.
[83] M. Davis, N.A. Hoult, A. Scott, Distributed strain sensing to assess corroded RC beams, Eng. Struct. 140 (2017) 473-482.
[84] F. Tang, H. Tian, H. Li, Monitoring steel bar corrosion based on distribution optical fiber sensing technology, Bridge Engineering Institute Conference 2019, Honolulu, Hawaii, USA, 2019.
[85] X. Li, W. Chen, Z. Huang, S. Huang, K.D. Bennett, Fiber optic corrosion sensor fabricated by electrochemical method, in: R.O. Claus, W.B. Spillman (Eds.), Smart Structures and Materials 1998: Sensory Phenomena and Measurement Instrumentation for Smart Structures and Materials, Spie-Int Soc Optical Engineering, Bellingham, 1998, pp. 126-133.
[86] L. Cai, W. Li, H. Fang, Characterization of Fe-C alloy film optical fiber corrosion sensors by fractal, in: Z. Cao, X.Q. Cao, L. Sun, Y.H. He (Eds.), Advanced Materials, Pts 1-4, Trans Tech Publications Ltd, Stafa-Zurich, 2011, pp. 976-980.
[87] C.K.Y. Leung, K.T. Wan, L. Chen, A novel optical fiber sensor for steel corrosion in concrete structures, Sensors 8(3) (2008) 1960-1976.

[88] K.T. Wan, C.K.Y. Leung, Durability tests of a fiber optic corrosion sensor, Sensors 12(3) (2012) 3656-3668.

[89] W. Hu, L. Ding, C. Zhu, D. Guo, Y. Yuan, N. Ma, W. Chen, Optical fiber polarizer with Fe-C film for corrosion monitoring, IEEE Sens. J. 17(21) (2017) 6904-6910.

[90] W. Hu, C. Zhu, X. Zheng, M. Gao, D. Guo, W. Chen, Polarization-based optical fiber sensor of steel corrosion, in: M. Razeghi, D.S. Temple, G.J. Brown (Eds.), Optical Sensing, Imaging, and Photon Counting: Nanostructured Devices and Applications, Spie-Int Soc Optical Engineering, Bellingham, 2015.

[91] F. Tang, Y. Chen, Y. Tang, G. Chen, Monitoring pitting corrosion growth in steel rebar using optical fiber, CORROSION2017, New Orleans, LA, USA, 2017.

[92] C. McCague, M. Fabian, M. Karimi, M. Bravo, L.R. Jaroszewicz, P. Mergo, T. Sun, K.T.V. Grattan, Novel sensor design using photonic crystal fibres for monitoring the onset of corrosion in reinforced concrete structures, Journal of Lightwave Technology 32(5) (2014) 891-896.

[93] V. Ramani, K.S.C. Kuang, Monitoring of rebar corrosion in concrete structures using a lens-based plastic optical fiber (LPOF) sensor, Constr. Build. Mater. 276 (2021) 15.

[94] M. Bravo, C. McCague, M. Fabian, L. Jaroszewicz, P. Mergo, M. Lopez-Amo, K.T.V. Grattan, T. Sun, Reinforced concrete structural corrosion monitoring using Hi-Bi photonic crystal fibres in a fiber loop structure, in: J.M. LopezHiguera, J. Jones, M. LopezAmo, J.L. Santos (Eds.), 23rd International Conference on Optical Fibre Sensors, Spie-Int Soc Optical Engineering, Bellingham, 2014.

[95] H. Wei, C. Tao, S. Krishnaswamy, Photonic crystal fiber based chloride chemical sensors for corrosion monitoring, in: T. Kundu (Ed.), Health Monitoring of Structural and Biological Systems 2016, Spie-Int Soc Optical Engineering, Bellingham, 2016.

[96] P.L. Fuhr, D.R. Huston, B. MacCraith, Embedded fiber optic sensors for bridge deck chloride penetration measurement, Opt. Eng. 37(4) (1998) 1221-1228.

[97] P.L. Fuhr, D.R. Huston, Corrosion detection in reinforced concrete roadways and bridges via embedded fiber optic sensors, Smart Mater. Struct. 7(2) (1998) 217-228.

[98] X. Zhao, Y. Cui, H. Wei, X. Kong, P. Zhang, C. Sun, Research on corrosion detection for steel reinforced concrete structures using the fiber optical white light interferometer sensing technique, Smart Mater. Struct. 22(6) (2013) 8.

[99] Y.F. Ma, Z.Z. Guo, L. Wang, J.R. Zhang, Probabilistic Life Prediction for Reinforced Concrete Structures Subjected to Seasonal Corrosion-Fatigue Damage, J. Struct. Eng. 146(7) (2020) 17.

[100] F. Tang, C. Li, H. Li, F.J. Presuel-Moreno, L. Fan, G. Chen, Probabilistic Evaluation of Service Life of Reinforced Concrete Beam Element in Marine Environment, CORROSION 2019, Nashville, Tennessee, USA, 2019.

[101] S. Lim, M. Akiyama, D.M. Frangopol, Assessment of the structural performance of corrosion-affected RC members based on experimental study and probabilistic modeling, Eng. Struct. 127 (2016) 189-205.

[102] K.A.T. Vu, M.G. Stewart, Predicting the likelihood and extent of reinforced concrete corrosion-induced cracking, J. Struct. Eng. 131(11) (2005) 1681-1689.

[103] C.Q. Li, W. Lawanwisut, J.J. Zheng, Time-dependent reliability method to assess the serviceability of corrosion-affected concrete structures, J. Struct. Eng. 131(11) (2005) 1674-1680.

[104] J. Mao, F. Xu, W. Jin, Q. Gao, Y. Xu, C. Xu, An Optical Fiber Sensor Method for Simultaneously Monitoring Corrosion and Structural Strain Induced by Loading, Journal of Testing and Evaluation 46(4) (2018) 1443-1451.